

6 Xenon and Cryogenics Systems

6.1 Introduction and overview of requirements

The functions of the xenon handling and cryogenics systems are to purify the xenon of the relevant contaminants, to condense it and to maintain it the liquefied state for the duration of the experiment, and to safely recover the xenon to permanent storage at the conclusion of the experiment.

Two classes of impurities drive the purification strategy.

1. Electronegatives such as oxygen or water limit the free electron lifetime and degrade the operation of the TPC. We require that the charge attenuation length of the LXe be 1.46 meters or larger, which is the maximum drift length of the detector. This corresponds to a free electron lifetime of 806 μ s at the drift field baseline of 310 V/cm (see Table 3.3.1), or an oxygen-equivalent concentration of 0.37 ppb. Electronegatives are removed from the xenon by continuously circulating the xenon in gas phase through a hot zirconium getter during operations.
2. Radioactive noble gases require special measures because they are not removed from the getter and because they create ER background events which can not be mitigated with self-shielding. Our primary concerns are ^{222}Rn and ^{85}Kr , but ^{39}Ar , ^{37}Ar , ^{220}Rn , and ^{127}Xe also play a role.

As detailed in Sections 9.7.1 and 9.7.2 background considerations imply that the vendor supplied xenon should be purified of $^{\text{nat}}\text{Kr}$ and $^{\text{nat}}\text{Ar}$ to the levels of 0.015 ppt (g/g) and 0.45 ppb (g/g)¹ respectively in order to suppress ER events from ^{85}Kr and ^{39}Ar . The krypton requirement is particularly demanding, and the need to control this species drives much of the xenon handling strategy.

At 0.015 ppt, the amount of krypton in the ten-tonne xenon stockpile is equivalent to 40 std-cc of air². To meet this requirement the xenon will be purified of both krypton and argon with a custom gas chromatography system at SLAC (see Section 6.3). Because no krypton removal technology will be employed during detector operations, it is critically important that krypton not be re-introduced once it has been removed. Air leaks and detector outgassing are two mechanisms of particular concern. This places additional burdens on the performance of the gas handling infrastructure and the operational protocols.

This chapter is organized as follows. In Section 6.2 we review the air leaks specifications of the purification and storage systems. In Section 6.3 we describe the SLAC chromatography system for removing krypton and argon. The online purification system and the xenon recovery systems are described in Section 6.4 and Section 6.5. The long-term xenon storage system is described in Section 6.6. The purity monitoring program is described in Section 6.7, and the cryogenics systems are described in Section 6.8. Xe procurement is described in Section 6.9, and some gas species diffusion and solubility measurements are reported in Section 6.10.

¹Unless otherwise specified, throughout this chapter we report concentration in units of (g/g). Concentrations of krypton and argon always refer to $^{\text{nat}}\text{Kr}$ and $^{\text{nat}}\text{Ar}$.

²The krypton concentration of air is 2.9×10^{-6} (g/g)

6.2 Xenon purification and storage specifications

In this section we describe the purification and storage specifications that bare upon the designs of the various xenon handling systems. Many of these specifications are driven by the the need to control the krypton concentration in the xenon. We adopt the following policy:

- the krypton removal system should produce xenon that has no more than 0.015 ppt (g/g) of krypton;
- the concentration should not increase more than 0.005 ppt/year while the xenon is contained in the storage system;
- the time-averaged increase in the concentration during five years of detector operations at SURF should be no more than 0.015 ppt (equivalent to 0.006 ppt/year).

6.2.1 Air leaks during storage

We estimate that the xenon will spend on average about six months in storage between krypton removal and delivery into the detector. If the above requirement is met, then the krypton content will not rise by more than about 0.0025 ppt from its initial value during this time. From the krypton concentration in air, we calculate that the allowed air leak rate into 10 tonnes is 0.017,3 g/y, equivalent to a helium leak rate of 1.15×10^{-6} mbar l/s (helium).³ ^{39}Ar will also contribute beta decay backgrounds in this scenario, however, due to its small abundance⁴ and longer half-life (269 vs. 10.7 years), its background burden is only 1.5 % of that of ^{85}Kr and is not constraining. Isotopes such as ^{222}Rn and ^{37}Ar are relatively short-lived (3.8 d and 35 d half-lives, respectively) and have a small enough concentration in air such that they are not a concern during long-term storage.

6.2.2 One-time air contamination during operations.

If a one-time xenon handling mistake introduces a small volume of air into the detector while running, the ^{85}Kr and ^{39}Ar decay rates will permanently increase, while ^{222}Rn and ^{37}Ar will also contribute unsupported ER backgrounds. The background burden from these species is as follows. We take the nominal ^{37}Ar concentration in air to be 1.2 mBq/m³ [3], and we take the Davis campus radon concentration as 300 Bq/m³. We assume that the quantity of dissolved air is 40 cc, and that the air is introduced near the beginning of the run. Then the number of ER events between 1.5 and 6.5 keV in the 5.6 tonnes fiducial volume in 1,000 days is 24.3, 2.3, 0.36 and 0.11 for ^{85}Kr , ^{222}Rn , ^{39}Ar , and ^{37}Ar , respectively. Here we have taken the branching fraction of the ^{214}Pb beta decay in the ^{222}Rn decay chain as being 9.2 %. ^{37}Ar contributes x-rays and Auger electrons to the ER band between 2 and 3 keV at a branching fraction of 90 %.

6.2.3 Continuous air leak during operations.

Here we assume that a continuous air leak exists in the Xe handling system during five years of underground operations, such that the long-lived isotopes ^{85}Kr and ^{39}Ar integrate continuously into the ten tonnes of Xe, and such that activity of ^{222}Rn and ^{37}Ar is now supported. We require that the average concentration of ^{85}Kr due to the leak lead to no more than 24.3 ^{85}Kr events, equivalent to the requirements on the krypton removal system. The average ^{85}Kr concentration is half the final concentration, and under these circumstances we find that the equivalent helium leak rate is 1.4×10^{-6} mbar l/s (helium), and the number of events due to ^{85}Kr ,

³We have used a conversion factor of one std cc-atm/sec (air) = 0.3722 std cc-atm/sec (helium).

⁴ $(^{39}\text{Ar}^{\text{nat}}/\text{Ar}) = 8 \times 10^{-16}$ (g/g) [1], while $(^{85}\text{Kr}^{\text{nat}}/\text{Kr}) = 4 - 23 \times 10^{-12}$ [2].

^{222}Rn , ^{39}Ar , and ^{37}Ar is 24.3, 0.51, 0.36 and 0.13 respectively (again taking the ^{222}Rn and ^{37}Ar concentrations in air as above).

6.2.4 Cosmogenic activation of the Xe

As detailed in Section 9.8.2, cosmogenic activation of the xenon during surface handling will result in tritium and ^{127}Xe activity in the Xe. After infinite exposure at sea level, the tritium decay rate would be about 30 decays/kg-day, or 1.7×10^8 decays in 5,600 tonne-days. Tritium is efficiently removed by the hot zirconium getter and is not expected to be problematic. GEANT4 predicts that the ^{127}Xe activity will be 2.6 mBq/kg in equilibrium at sea level, and detector simulations show that the rejection factor of all selection cuts will be 1.1×10^{-5} . Therefore we require that the initial activity be reduced to 88 mBq/kg at the start of physics data taking so that no more than 23 ER events remain after cuts. This implies a 178 day cool-down period underground, which is comparable to the detector commissioning time and is acceptable.

6.3 Krypton Removal via Chromatography



Figure 6.3.1: The three panels show the Kr removal development platform. Left: the gas control manifold, pumps, and charcoal column. Center: LN thermosyphon cooled condenser for xenon recovery. Right: krypton traps and xenon feed and storage located on the back side of the manifold.

Commercially available research-grade Xe typically contains trace Kr at a concentration up to 100 ppb (parts per billion). ^{85}Kr is a β -emitter with an isotopic abundance of $\sim 2 \times 10^{-11}$ in natural Kr [1], an endpoint energy of 687 keV, and a half-life of 10.8 years. To reduce the rate of ^{85}Kr ER backgrounds to 10 % of the *pp* solar neutrino ER rate, we require that the total concentration of Kr be no more than 0.015 ppt (parts per trillion), equal to a reduction of up to $\sim 10^7$ below that of research-grade Xe. Since the Kr is dissolved throughout the Xe, ^{85}Kr decays cannot be rejected via self-shielding, nor does the getter remove Kr during *in situ* purification, due to its inert nature. Gas vendors have indicated that they could guarantee Xe with a Kr concentration as small as 1 ppb at additional cost, however this would still far exceed the LZ background goal. As noted in Section 6.9, 20% of the Xe for LZ has been received and assayed, and all of it meets or exceeds spec.

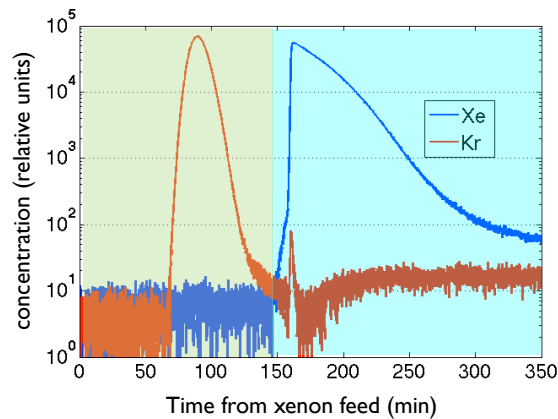


Figure 6.3.2: Test data taken with the LUX Kr removal system illustrate the time profiles for Kr and Xe as they exit the column for a sample of xenon spiked with approximately 1% krypton. Data are acquired with a sampling RGA. During production, the ~ 100 ppb Kr in the raw Xe is below the RGA sensitivity so spiked samples are used to tune the chromatography parameters.

Trace Ar is also a concern due to the presence of the β -emitter ^{39}Ar (endpoint energy of 565 keV and half-life of 269 years), and we require that the background rate due to ^{39}Ar be no more than 10% of that of ^{85}Kr . Due to the low isotopic abundance of ^{39}Ar (8×10^{-16}) [1], this implies an Ar concentration requirement of 4.5×10^{-10} (g/g), substantially less demanding than the krypton requirement. Furthermore, because Ar is amenable to the same removal techniques as Kr, no special measures are required to satisfy the Ar goal. Likewise, no special assays are required, since our technique simultaneously measures the residual Ar concentration along with the Kr.

LZ will employ gas charcoal chromatography to remove Kr and Ar from Xe using the process that we successfully developed and executed for XENON-10 [4] and LUX [5]. The method employs a charcoal column with a continuously circulating He carrier gas and exploits the different transit time through the column for the various gas species. The weaker van der Waals binding of Kr to activated charcoal relative to Xe causes Kr atoms to flow through the charcoal column more rapidly than Xe. This property allows for a separation cycle by feeding Xe (with trace Kr) into the column at a fixed rate and duration under the influence of the fixed carrier flow. The rate and duration are tuned so that the last of the Kr exits the column prior to the earliest Xe. This permits the Kr to be purged by directing the Kr-He stream to a coldtrap that captures the Kr. This feed-purge cycle is followed by the Xe recovery cycle, in which pumping parameters are altered to accelerate the rate at which the Xe exits the column.

Figure 6.3.2 illustrates this process by showing the time profiles for the two species as they exit the column. The Kr-He exits first during the chromatography cycle to achieve Xe-Kr separation. Then, as the purified Xe-He stream exits the column, the Xe is frozen out from the stream using a cryogenic condenser, while the He circulates until recovery is complete. After a number of feed-purge-recovery cycles, the He is pumped away, the condenser is warmed, and the Xe is transferred to a storage cylinder. The purity of the Xe is measured using the coldtrap/mass-spectrometry technique developed at Maryland [6] and described in Section 6.7.

Using this method, the SLAC group, while still at Case Western, processed the 400 kg of LUX Xe at a rate of 50 kg/week down to a Kr concentration of 4 ppt, exceeding the LUX goal of 5 ppt and rendering this background sub-dominant to the leading background by a factor of 10 during the 2013 LUX WIMP search [5, 7]. The starting concentration was 130 ppb of Kr and the typical batch reduction factor was 3×10^4 . In addition, one 50 kg batch of Xe that was “spiked” to approximately 0.01% Kr was processed twice, resulting in an upper limit on the concentration of 0.2 ppt, which was our assay sensitivity at that time. This powerful

reduction of 9 orders of magnitude resulted in Xe with a Kr concentration only a factor of 13 higher than the ultimate LZ goal, and shows that sequential processing gives multiplicative reduction and is a suitable method to achieve clean Xe for LZ.

While this result is encouraging, it demonstrates only that cross-contamination of feedstock to recovered Xe can be mitigated by multi-pass processing. However, reaching the LZ goal also requires that sources of contamination and ingress of Kr-laden air also be controlled down to the ultimate required concentration. To ensure that our method is sound, we reconfigured the LUX production system as a development platform, which is shown in Figure 6.3.1. We have been using that system to refine our process and have learned several valuable lessons that are being incorporated into the production system including: the pre-scrub of the He carrier gas through a cold-trap to remove trace Kr prior to use for purging of the primary traps; the placement of the Kr trap as close as possible to the charcoal column to mitigate contamination from upstream components; the gradual turn-on of Xe into the feed cycle to avoid pressure spikes and backflow into the output side of the Kr trap, which otherwise results in cross-contamination; the importance of all-metal seals throughout the system; and the critical nature of the Xe recovery pump, which is the most complex component through which the purified Xe passes. In addition, we have used the assay system to prepare 100-gram samples of highly-purified xenon that we backflow into various parts of the system, recover, and assay to see if the xenon remains pure. We expect to make significant use of this powerful diagnostic tool to isolate, identify and mitigate deficiencies in the production system, as we have done in the R&D system. Each of the lessons learned has resulted in progress in bringing down the level of the Kr, which in our best batches to date is 0.075 ppt. At the time of this writing, we await the arrival of an improved Xe recovery pump with better isolation between the process space, the internal gearbox, and the external environment.

In addition to purity requirements, the processing rate and duration of a production run also influence the design of the full LZ system. Figure 6.3.3 provides a simplified schematic of our design for the production system, which will process 200 kg of Xe per day, or 10 tonnes in 60 days at 85 % uptime. This design has better isolation between the chromatography loop and the recovery loop than did the LUX design, which achieved 3×10^4 reduction per pass and was likely limited by cross-contamination. While we may expect some improvement of the Kr rejection factor as the system is tuned during initial operations, we conservatively plan for two complete passes of the Xe (120 days), which is more than sufficient to reduce the Kr concentration in the raw stock by a factor of 10^7 . Fast processing also provides schedule insurance in the event of an unintentional contamination event. We note that the introduction of just 40 cm^3 of air at standard temperature and pressure (STP) corresponds to 0.015 ppt of Kr in 10 tonnes of Xe. A single pass through the chromatographic system could easily correct an error as large as hundreds of liters. (The corresponding requirement for argon is less demanding: 270 cm^3 of air at STP.)

As illustrated in Figure 6.3.3, the three principal processing stages are: (1) chromatography to separate Xe and Kr, and capture the Kr in a cooled charcoal trap; (2) recovery of the Xe from the column into a cooled condenser to strip the Xe from the carrier gas; and (3) storage and analytical sampling of the purified Xe into LZ storage packs for transport to the experiment. The system architecture follows two general principles. First, we minimize the components exposed to both the raw and purified Xe streams to minimize cross-contamination, which leads to the two mostly separate loops in the figure (green and blue). Second, the arrangement matches the feed-purge cycle time to the Xe recovery time, so that by alternating between the two columns, we achieve twice the duty cycle of single-column operation. Two condensers are also used so that one is always available in the recovery path when the other is in the storage phase. The double-swing system with two columns and two condensers gives a factor-of-4 increase in production rate relative to a single-column-single-condenser system at modest additional cost and complexity. Moreover, reduced labor for the shorter production run more than offsets the incremental hardware cost of the second condenser and column.

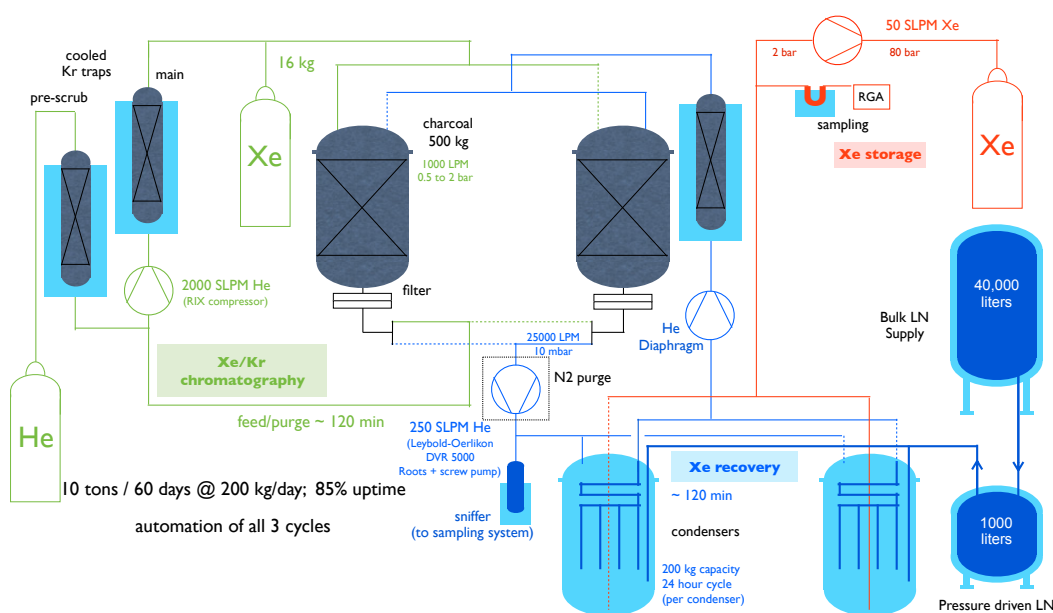


Figure 6.3.3: This figure shows the main components and flow paths of the LZ Kr removal system. Colored lines indicate the path for a given process. The green line shows the left-hand charcoal column in the chromatography feed-purge separation cycle with Kr being collected in the right trap; a second trap is valved out for cleaning (dashed green line). The blue line shows the subsequent part of the cycle in which Xe is being recovered from the column and collected in the condenser. The red line shows Xe from the condenser being stored and analyzed. Key pressures and flow rates are indicated.

The overall processing rate is governed by the differential transit time of the Kr and Xe in the column, whereas all other components are sized to match this rate. In the LUX system, each feed cycle consisted of a 2 kg slug of Xe into a column of 60 kg of charcoal at 50 slpm⁵ He flow rate. The Kr purge was completed 120 minutes after the start of the feed, at which time recovery commenced. Straightforward scaling to reach 200 kg per day calls for a 16 kg-slug every two hours, which in turn requires an approximate eight-fold scaling in charcoal mass and flow rate. Some additional tuning will be required based on further studies of chromatography and cross-contamination using the LUX system. The remaining parameters, as shown in Figure 6.3.3, are appropriately scaled from the existing system.

The system architecture uses computer-controlled pneumatic valves for changing all of the process states between the various cycles. Pumps, mass flow controllers, heaters, and diagnostic sensors (pressure, temperature, etc.) are controlled and/or read out by this system as well. We will use programmable logic controllers (PLCs) for process control since they are a standard industrial solution that is robust and gives low latency for reliable control and system interlocks. The PLC system will interface with the SCADA software package Ignition, by Inductive Automation, which we have been using in the R&D system. The three primary cycles (chromatography, recovery, storage), as well as Kr trap cleaning and analytic sampling, will be fully automated, minimizing the chance of operator error.

The Kr-removal system uses a cryogenic condenser system to freeze the purified Xe out of the Xe-He stream at LN temperature. A schematic of the combined condenser and LN system is shown in Figure 6.3.4. The design of the condenser is based on the LUX approach with several new features that will simplify construction and operation, and reduce cost. A set of LN-cooled surfaces mounted in a pressure vessel accumulates the purified xenon. After a number of runs, the He is evacuated, the system is warmed to LXe

⁵standard liters per minute

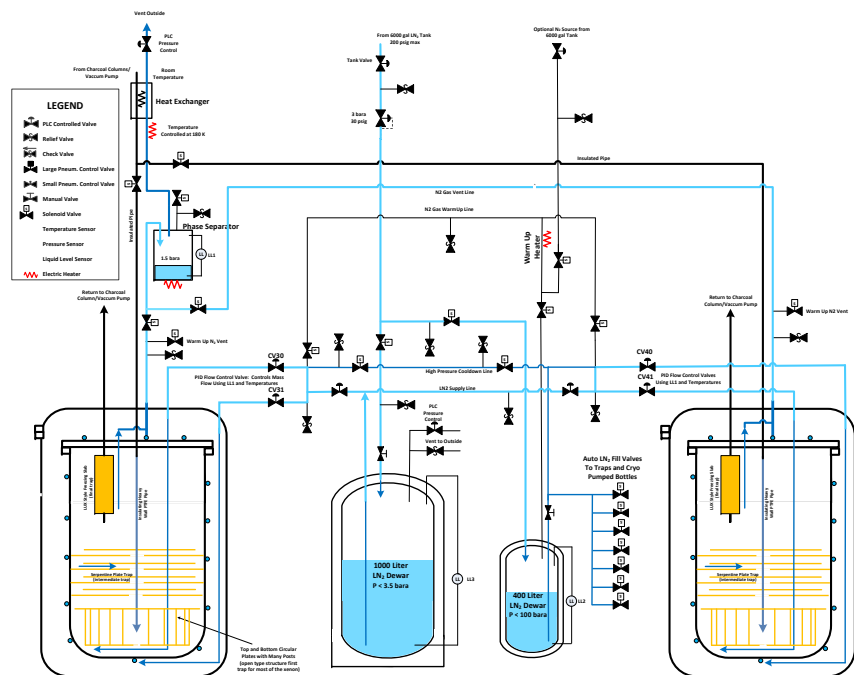


Figure 6.3.4: A schematic of the condenser and LN distribution system. One condenser is alternately coupled to the two charcoal columns, with LN supplied by the 1000-liter pressurized storage dewar, 1-2 days of recovery cycles. During that time, the other condenser is in the warming, storage, and re-cooling cycle. The 400-liter LN dewar supplies cryogenics for rapid recooling as well as the various LN-cooled traps. The two LN dewars are resupplied by the 9,000 gallon tank at IR2 (not shown).

temperature, and the xenon is compressed into LZ storage packs for either a second pass or transport to the experiment. The Kr removal system will use one of the storage compressor skids described in Section 6.5, which will then travel to South Dakota with the processed xenon. Since we don't require precision temperature control as in a LXe detector, rather than using a more complex thermosyphon system to provide cooling we have designed a simpler force-flow system. This system will deliver LN through a system of copper tubes that are brazed to the vessel walls and internal structures. The direct LN cooling will easily meet peak load and rapidly recool the vessels after storage of a previous batch. The pressure-driven LN loops will consist of long circuits of copper piping that will be coupled to a series of copper plates in the condenser space and to the outer wall of the vessel. Because cooling power can be better distributed than with individual thermosyphon cold heads, the design will have a favorable ratio of xenon capacity to vessel size. Finally, the pressure-driven LN system has fewer control points than the thermosyphon and will be more straightforward to program and operate. A detailed engineering note contains a through analysis of the time-dependent heatload defined by the variable rate of the Xe recovery (Figure 6.3.2), as well as the reduction in cooling power as frozen Xe accumulates (Xe ice is a poor thermal conductor).

In Figure 6.3.5, we show a physical layout of the major system components, including pumps, columns, condensers, traps, pressure-driven LN supply, and sampling subsystems. The system will be installed in Building 624 at the IR2 complex at SLAC. The Xe, which is a high-value asset, will be stored in a locked "sea container" in front of the pad. Not shown is the nearby LN storage tank, which is refilled by truck under SLAC contract.

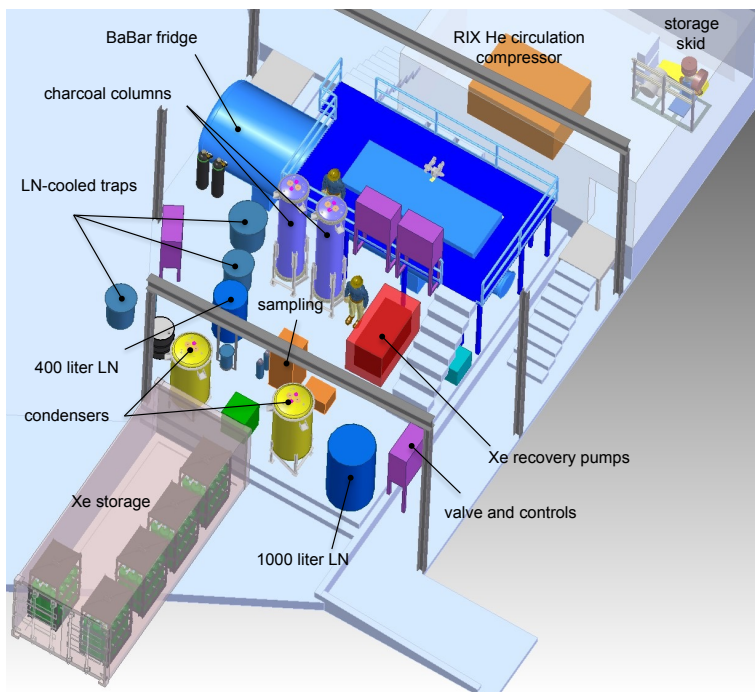


Figure 6.3.5: A layout of the LZ Kr removal system shows all major components located at the former BaBar LHe cryopad in building 624 at the SLAC IR2 complex. If a buyer for the refrigerator is not found, this layout shows the adequacy of the remaining space. The partial soft-wall exterior is well suited to mitigate oxygen deficiency hazard with the large quantity of cryogenics in use. A 20-foot sea container at the front of pad will provide secure storage for Xe cylinder packs and ease in handling.

A high-flow-rate RIX 2-stage piston pump for circulating the carrier gas during chromatography has been identified at SLAC and is available for LZ. The purity requirements of this pump are modest because the He will pass through the LN-cooled charcoal trap prior to the Xe feed branch and the chromatography columns.

As noted in the R&D discussion, the Xe recovery pump system is the most complex component that sees the purified xenon. We have worked closely with Leybold-Oerlikon to evaluate commercially available dry pumping systems. We provided the manufacturer with a fully-detailed data set rescaled from our LUX slow control data, including He and Xe pressures and mass flow rates for the full recovery cycle. The manufacturer has used their proprietary software to make a detailed assessment of pump performance, and determined that a stock version of the DVR 5000, which combines a dry Roots booster backed by a dry screw pump will meet our requirements.

During processing, several hundred kilograms of Xe will be in various parts of the system. To protect against loss of Xe we will rely on backup systems to maintain cooling power. Short-term outages are protected by UPS units. For longer outages, the SLAC operations team has deployed a standby generator that will come online within 1 to 2 minutes. These capabilities will allow the control systems to replenish the LN₂ reservoirs in the Kr removal system from the nearby 9,000 gallon LN storage tank at the IR2 complex.

A fully-detailed P&ID⁶ has been developed for the production system. The design is based on the principles of the LUX system that was reconfigured for R&D, while following the overall architecture shown in Figure 6.3.3. The production system P&ID is shown in Figure 6.3.6.

⁶Piping and Instrumentation Diagram

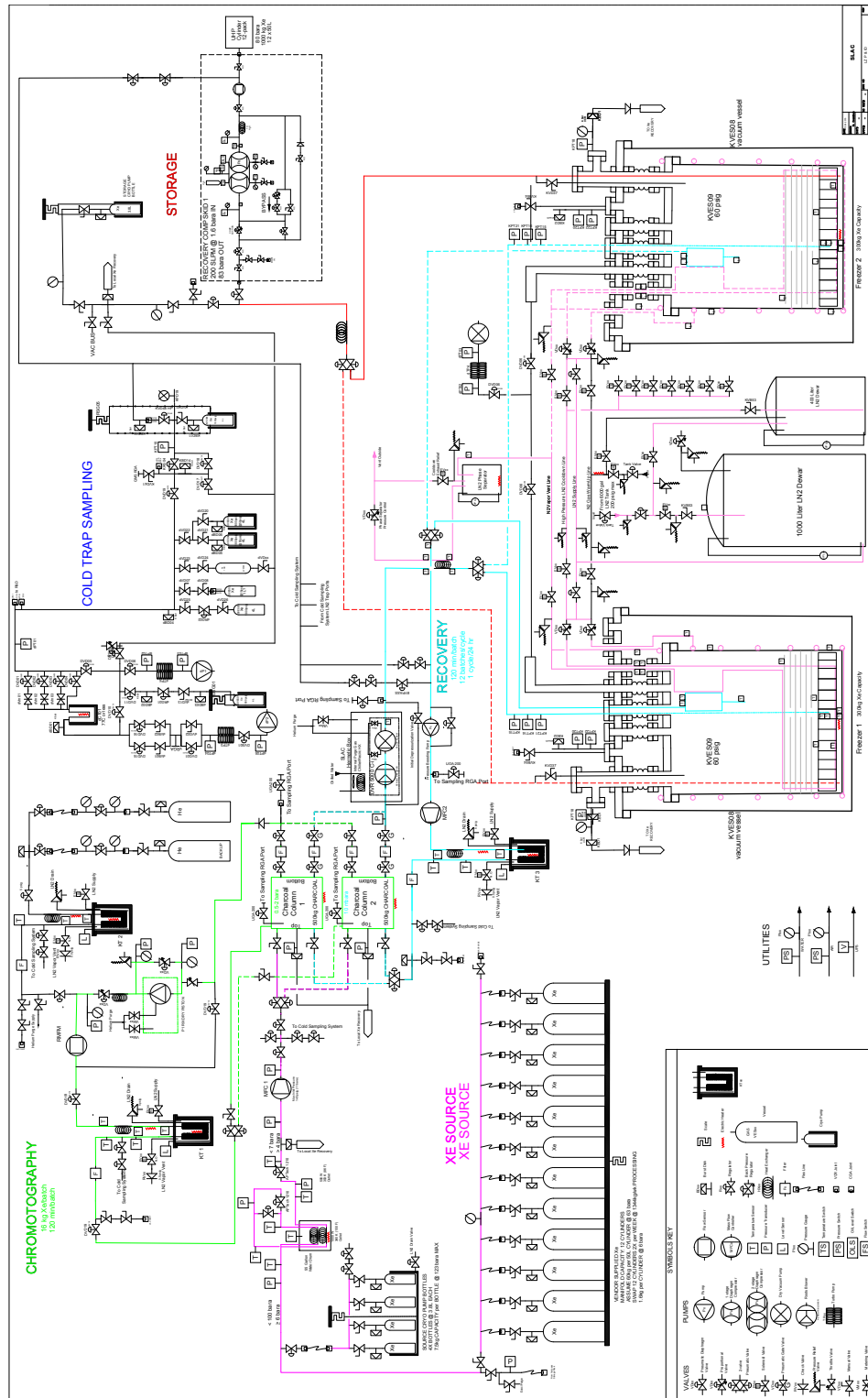


Figure 6.3.6: The P&ID for the LZ Kr removal system.

6.4 Online Xenon Purification System

This section describes the online Xe purification system, which controls the concentration of electronegative impurities such as O_2 and H_2O during detector operations through continuous purification. The system is shown schematically in Figure 6.4.1. Liquid xenon is removed from the detector at the weir trough near the top of the TPC. The design flow rate is 500 slpm (2.8 kg/min), or about 1.0 l/min. The liquid exits the cryostat and flows to the LXe tower through vacuum insulated transfer lines that penetrate the water tank. In the LXe tower it is evaporated, compressed to higher pressure, is purified, and then recondensed and returned to the detector.

A central feature of this design is a set of two heat exchangers located in the LXe tower that make the phase and temperature change thermally efficient. Without these heat exchangers, 4.3 kW would be required in each flow direction at 500 slpm for the phase change alone.

This section is organized as follows. The gaseous portion of the circulation system is described in Section 6.4.1. The LXe tower and the vacuum insulated transfer lines are described in Sections 6.4.2 and 6.4.3. We report on results from a prototype circulation system that implements the LZ architecture in Section 6.4.4. A radon removal system that treats the gaseous xenon in the breakout box and cable conduits is described in Section 6.4.5, and the slow controls is described in Section 6.4.6.

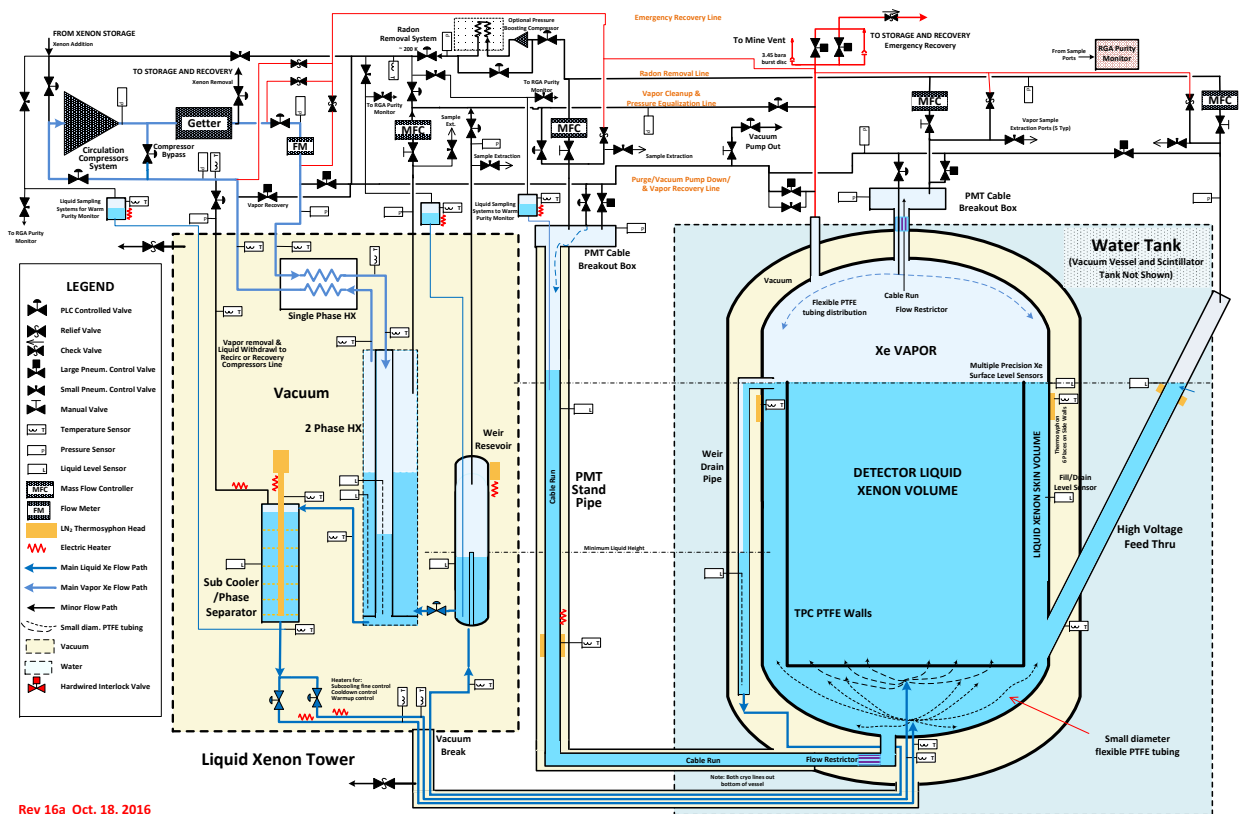


Figure 6.4.1: Overall flow diagram of the LZ online purification system. The shaded box on the left represents the LXe Tower, where the phase changes between LXe and GXe occurs. The top of the diagram represents the gas recirculation system. Note that this figure captures the design at a high level, but the master P&ID should be relied upon for details.

6.4.1 Gas recirculation system

The Xe gas recirculation system receives gaseous xenon from the detector via the LXe Tower (Section 6.4.2), circulates the xenon through the hot zirconium getter to remove electronegative impurities, and returns the purified Xe to the LXe Tower. This system also handles Xe purge flow and Rn-Removal (Section 6.4.5) to/from the detector cable conduits, as well as calibration source injection. A complete P&ID for this sub-system is provided in Figure 6.4.2.

The centerpiece of the LZ online purification system is a hot zirconium getter (model PS5-MGT100 from SAES), a purifier technology capable of achieving >99 % one-pass removal efficiency for virtually all non-inert impurities of interest, including hard-to-remove species such as N₂ and CH₄ [8]. Impurities chemically bond to the surface of zirconium pellets, irreversibly removing them from the Xe. The getter operates at elevated temperature (450 °C) to allow the captured impurities to diffuse into the bulk of the getter pellets, leaving the surface free for additional getting. The getter material must be replaced when it becomes saturated with impurities. The SAES getter comes equipped with valves, plumbing, controls, and an engineered integrated safety interlock system that will disable the getter power and isolate the getter from the process gas in the event that excessive heat is detected.

The Xe circulates through the purification system at a rate of 500 slpm (2.8 kg/min), a value that was chosen based upon previous experience with the LUX system and based on economic and space constraints. At this flow rate, the 10 tonnes of Xe can be purified in 2.3 days, comparable to the 1.7-day turnover time of the LUX recirculation system. The recirculation rate and the charge attenuation goal constrains the allowed outgassing rate of the detector, and this drives the outgassing plan of the detector. Prior experience with LUX and other liquid noble detectors indicates that the scintillation absorption length goal (>15 m) is less demanding than the charge attenuation goal and will be satisfied by the same requirements.

Circulation through the purification system is provided by a set of all-metal triple-diaphragm two-stage compressors. This type of compressor uses an electric motor to drive single-piston oil pumps that pressurize the bottom diaphragms of each stage, transmitting force to the top diaphragms to compress the gas. Middle diaphragms with grooves create a space that is monitored for leakage of either oil or Xe. The all-metal design (including metal main head seals) minimizes the ingress of krypton and radon into the Xe. A 100 slpm Fluitron compressor of this type and utilizing this all-metal seal technology has been operating at SLAC as part of the System Test (Figure 6.4.3), allowing us to begin building a strong understanding of operating performance, characteristics, leak-tightness, and maintenance. For LZ, two compressors, each rated for 300 slpm at 1 bara suction pressure and capable of 10 bara output pressure, operate in parallel to provide the full system flow. Together these compressors nominally deliver 600 slpm of flow, so a proportional control valve modulates excess flow back to compressor suction to maintain the nominal 500 slpm circulation through the purification system. Scheduled maintenance (every 5,000 hours) and unexpected repairs on these machines will require periodic operations at reduced circulation rate (approximately 300 slpm from the remaining online compressor).

After-cooling of the compressed gas may be adjusted so preheated gas can be delivered to the getter. Hot gas exiting the getter is cooled back to room temperature by a heat exchanger provided with the getter. The purified gas is then returned to the LXe Tower. The online sampling system (Section 6.7) has taps to draw samples from upstream of the compressor, and upstream/downstream of the getter. Xenon that has already been sampled reenters the circulation loop downstream of these taps.

The gas plumbing for the recirculation system is pre-cleaned stainless steel (SS) tubing connected with lanthanated or ceriated orbital welds wherever possible. VCR fittings with metal seals will be used where necessary to open a connection. Valves will be of the bellows- or diaphragm-seal type to keep the system hermetic. Gas panels will be sealed to allow for panel-wide He leak checking during testing and commissioning, as well as continued N₂ purge during operations.

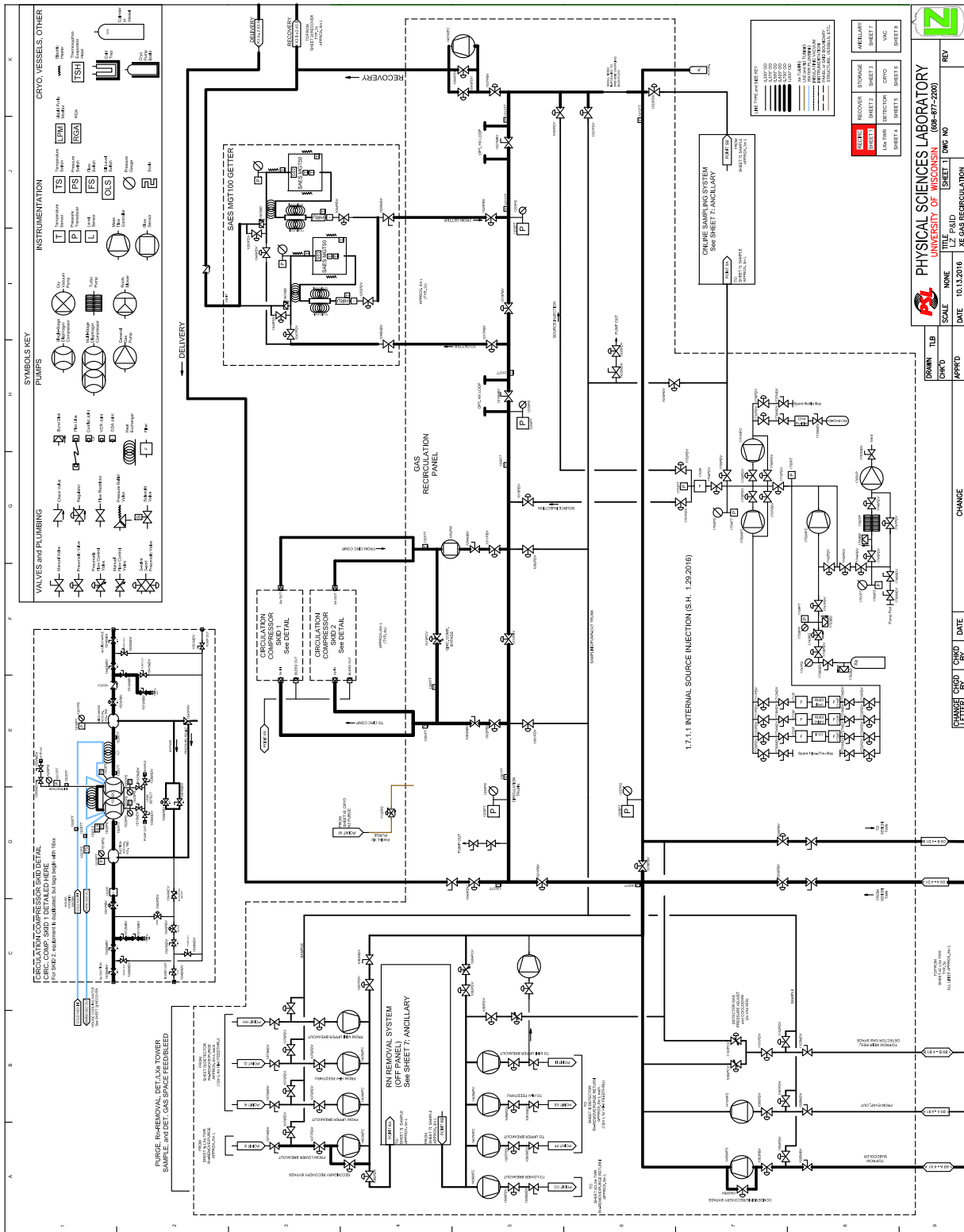


Figure 6.4.2: Xe Gas Recirculation system P&ID.



Figure 6.4.3: Fluitron 100 slpm all-metal single-stage diaphragm compressor operating as part of SLAC System Test.

In addition to the primary Xe recirculation path, four secondary gas-only recirculation loops act on the detector conduits that house the cables for the PMTs and instrumentation cables (from Xe vessel top and the PMT standpipe). These cables are immersed in LXe on one end, but they penetrate the liquid surface and terminate at room-temperature feedthroughs filled with Xe gas at the other end. These cable bundles are a potential source of problematic outgassing, particularly the warm ends where the diffusion constants of the insulating plastics are the largest. We manage this outgassing by purging these conduits with a continuous flow of Xe gas away from the TPC at a modest flow rate. This purge gas flow merges at the input of the online Rn-removal system (Section 6.4.5), and then returns back to the conduits, bypassing the LXe tower. Purge flow is driven by a small independent gas compressor in the Rn-Removal system. Plumbing provisions also allow for a portion of the Rn-Removal system output flow to be directed into the main circulation loop to create a purge flow imbalance and provide evaporative cooling to the conduits if desired. The purge-gas flow rate required to ensure that back-diffusion is negligible is characterized by the unitless Peclet number, $P = VL/D$, where V is the linear velocity of the gas in the conduit, L is the diffusion distance of interest, and D is the diffusion constant of the impurity species. For a 4 inch diameter conduit, a gas flow rate of 0.5 slpm per conduit, a diffusion distance of 10 cm, and a diffusion constant of $0.086 \text{ cm}^2/\text{s}$ (valid for O_2 diffusion in Xe gas at room temperature), the Peclet number is 8.2, indicating that back diffusion is negligible. We plan for a total of 2.0 slpm of flow across all conduits (three cable conduits and one high voltage feedthrough conduit). Figure 6.4.4 is a portion of the P&ID detailing the detector, which shows how these purge paths are tied into the detector conduits. LXe paths are on bottom, GXe taps are above the LXe level.

The circulation system must also accommodate detector calibration and purity assays. As discussed in Chapter 7, radioactive sources such as $^{83\text{m}}\text{Kr}$ and tritiated methane will be introduced into the Xe to calibrate the central regions of the TPC, and the online purification system has a valve and port system to allow for this. Due to its inert nature, $^{83\text{m}}\text{Kr}$ may be injected into the circulation stream upstream of the getter, whereas tritiated methane must be injected downstream. There are also valves to allow for the sampling of the LXe in the tower and gaseous Xe before and after the getter, as described in Section 6.7. Details of the source injection plumbing and how it ties into the gas recirculation system can be found lower-center in Figure 6.4.2.

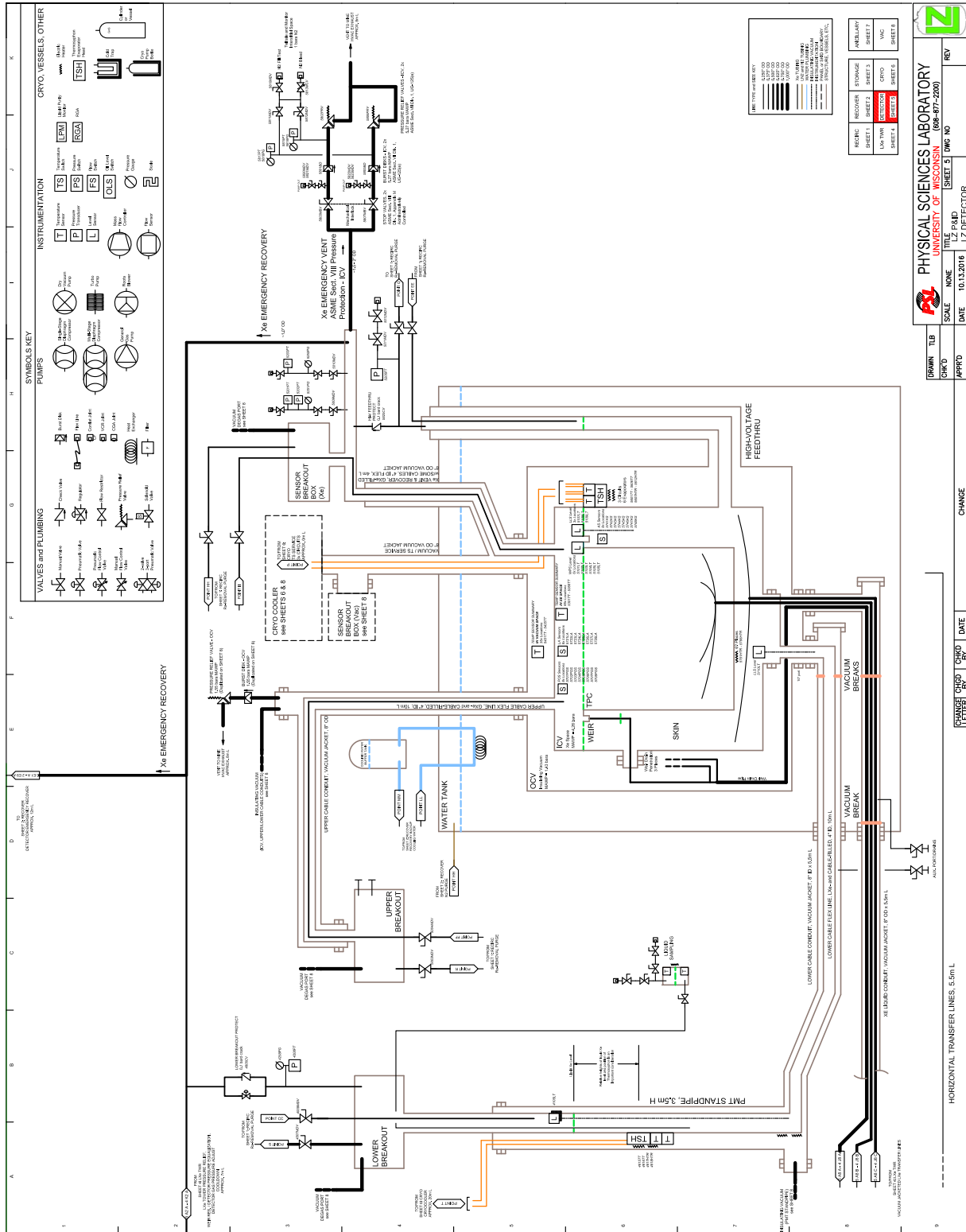


Figure 6.4.4: P&ID of Detector and Xenon Handling Tie-Ins.

6.4.2 Liquid xenon tower

Because the hot getter in the purification system (Section 6.4.1) operates on gaseous Xe (GXe) only, the purification system must vaporize and re-condense the liquid Xe (LXe) to create a continuous purification circuit. This process is made thermally efficient by using counter flowing single- and two-phase heat exchangers in series with a sub-cooler/phase-separator within the LXe Tower assembly. The Xe is transferred in liquid form between the LXe Tower and the detector through vacuum-insulated transfer lines that penetrate through the wall of the water shield and connect to the bottom of the TPC vessel.

The LXe Tower is shown in detail in Figure 6.4.5 and contains the following major components: 1) a valve block that houses LXe flow control and LXe Tower isolation valves; 2) a weir reservoir for collecting the liquid returning from the detector and preparing it for evaporation; 3) a counter flow serial two-phase and single-phase heat exchanger assembly for evaporating the LXe and bringing the exiting GXe to room temperature while pre-cooling the returning GXe and liquefying the xenon gas; 4) a subcooler/phase separator for cooling the return liquid and removing gas bubbles; and 5) three thermosyphon heads; three liquid sampling ports. The LXe Tower P&ID is shown in Figure 6.4.6.

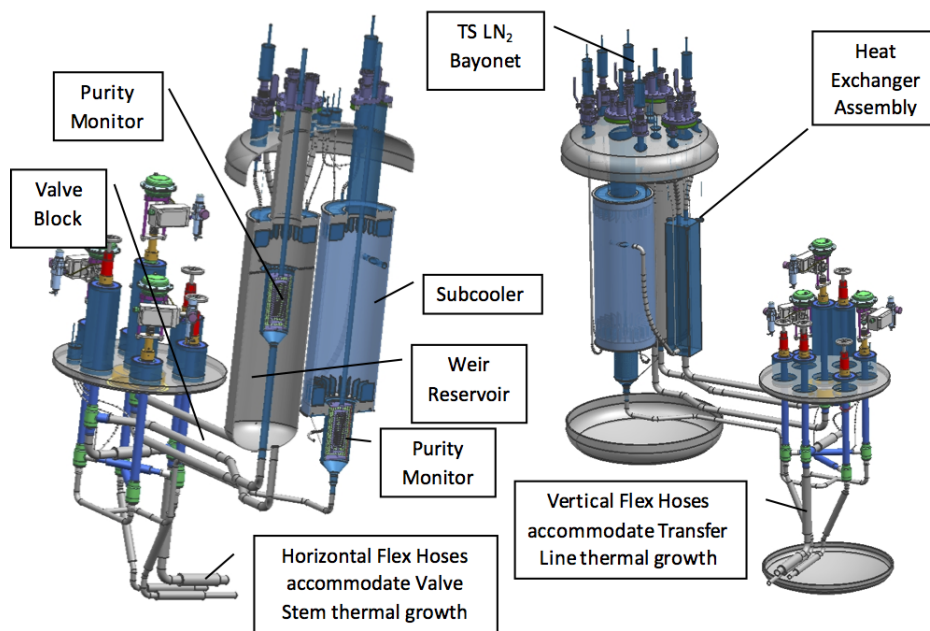


Figure 6.4.5: Two views of the LXe tower assembly. The heat exchanger assembly is visible in the right image and the subcooler and weir reservoir components can be seen at the left. The cryogenic valves are consolidated in a separate valve block (visible in both views) to provide easy access to the actuators and also to allow for isolation between the LXe tower and the detector.

In addition, the tower design includes space for two optional liquid purity monitors, one located in the inlet to the weir reservoir, to measure the purity of the xenon on the way out of the detector, and the other located in the subcooler, to measure the purity of the xenon entering the detector. Cryogenic components will hang from the top of the vacuum jacket to allow for fabrication with the vacuum jacket removed. When the internal structure is complete, the vacuum jacket is welded shut on the sides and bottom. There is a vacuum break at the bottom of the xenon tower isolating its vacuum from the detector for safety considerations and for LN₂ checkout.

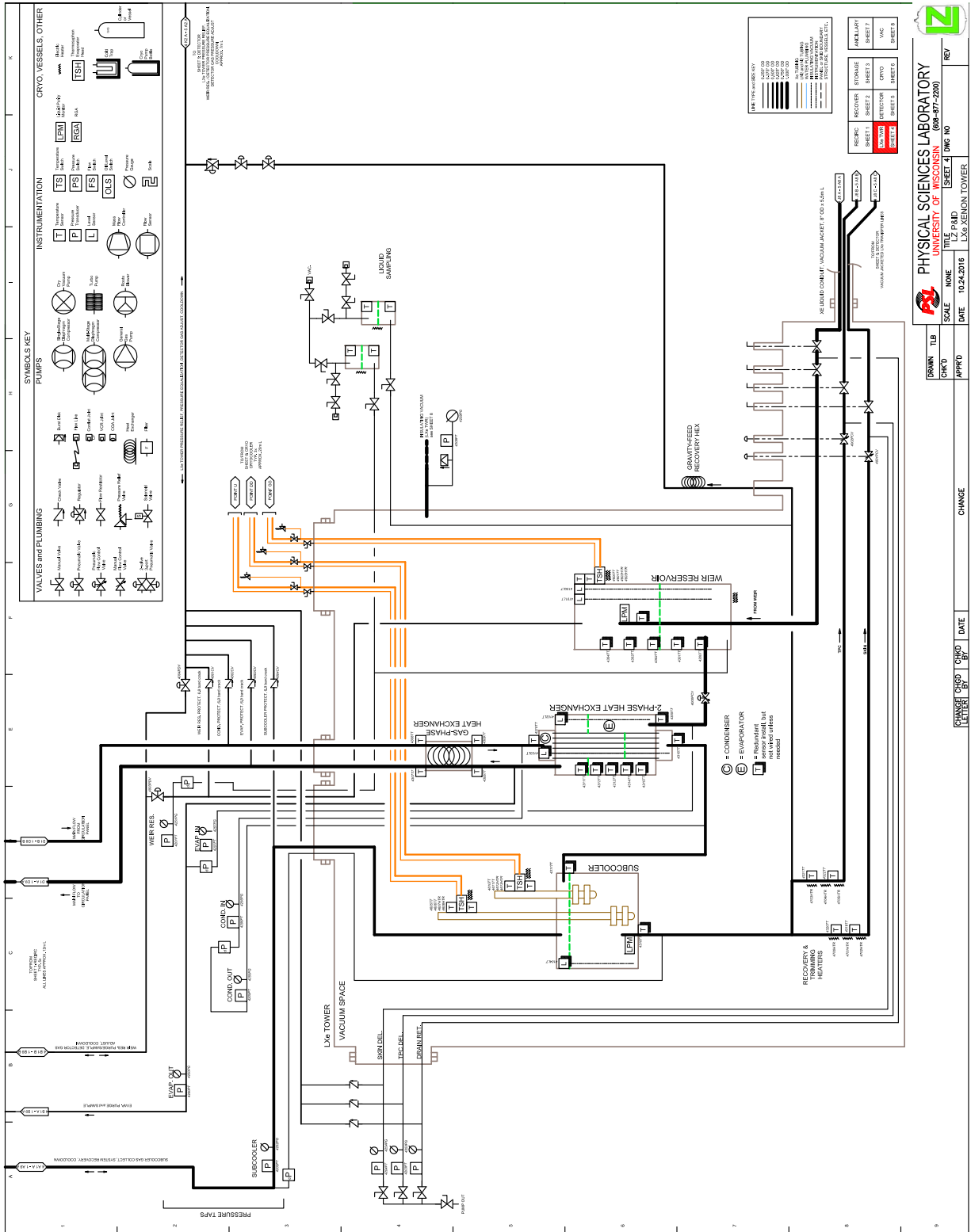


Figure 6.4.6: P&ID of the LXe Tower.

Liquid flow from the subcooler passes through two sets of two cold control valves that partition the flow between the TPC volume and the skin volume. Each valve set is paired to allow the LXe tower to be isolated from the detector. These valves will be used during normal operation, for vessel cool-down, and for changing flow rates and patterns during injection of radioactive Kr and methane. Both of these flow streams have an electric heater with thermometer for cool-down and warm-up control. These valves are also used for liquid extraction to compressor suction during warm-up. A third pair of cold control valve is placed between the weir reservoir and the evaporator side of the two-phase heat exchanger. This valve set works in conjunction with the compressor suction control to establish the height of the boiling LXe. It will also provide a small amount of Joule-Thomson cooling by using the energy supplied from the recirculation compressor. All three of these cold control valve sets are bellows sealed and designed for use in helium liquefiers.

The weir reservoir is a simple 35.6 cm diameter ASME stamped vessel that acts as a volume buffer between the weir drainpipe and the two-phase heat exchanger. LXe flows down the weir drainpipe in the detector, through the transfer line, and up the weir reservoir standpipe. Besides establishing the liquid level in the weir drainpipe in the detector, the weir reservoir also provides a location to collect nonvolatile impurity species that may be present in the LXe. Such species, if they exist, would become harmlessly trapped in the weir reservoir. A liquid sample tube from the weir reservoir liquid sampling system to the bottom of the weir reservoir makes it possible in principle to remove contamination.

Liquid flows from the bottom of the weir reservoir into the bottom (evaporator) of the two-phase heat exchanger where it is vaporized, while Xe from the getter is condensed. The bottom of the weir reservoir is placed at a relative height above the bottom of the two-phase heat exchanger to provide a small liquid pressure head to push fluid into the heat exchanger. Liquid is also drawn up into the evaporator side of the two-phase exchanger by the lower pressure of the suction side of the gas compressor. As LXe flows from the bottom of the weir reservoir into the bottom of the heat exchanger assembly, the LXe undergoes a phase change (vaporization) into GXe on the evaporator side while GXe from the getter changes to LXe in the condenser side of the assembly. The mass flow rates are the same for each circuit of the heat exchange assembly, during steady state operation. The condensing side operates at a higher pressure than the evaporator side, and because the heat of vaporization is higher at higher pressure, any excess energy released during the phase change evaporation process can be used to sub-cool the LXe after condensation and before entering the sub-cooler/phase separator.

Both the single-phase and two-phase heat exchangers will be commercial plate heat exchangers which have a high heat transfer efficiency relative to their physical footprint. Because the single-phase and two-phase heat exchangers are of similar style, they are combined into a single heat exchanger package which houses both the gas to gas and phase change heat transfer. As discussed in Section 6.4.4, data from the LZ System Test are being used to ensure that the system conditions that affect heat exchanger design are understood. These system conditions include the relative liquid heights within the system and the inlet and outlet temperatures and pressures.

Any additional heat exchange assembly inefficiencies and thermal loads on the LXe are removed before the liquid enters the detector in the subcooler, the last major component of the LXe tower. The subcooler, or phase separator, is made with perforated copper plates attached to a central copper rod with thermosyphon heads at top or bottom. Copper mesh or similar will be placed between the copper plates (depending upon analysis) to ensure a more than adequate heat transfer area. During normal detector operation the subcooler serves two purposes. Any xenon vapor not condensed by the two phase heat exchanger can separate from the liquid flow in the ullage of the subcooler and be condensed, and the liquid itself can be sub-cooled before it enters the detector cryostat as required. The refrigeration of the cryostat can be optimized by adjusting the power of the subcooler thermosyphons and the detector cryostat thermosyphons. Using the nominal detector vapor pressure of 1.8 bara, the bottom of the detector has a pressure of 2.25 bara, translating to a saturation temperature of 180.3 K. A thermosyphon is able to reduce the liquid xenon temperature close to the freezing

point 161.5 K. The temperature of the sub-cooled xenon can therefore be adjusted to make up any heat loads on the TPC space. The skin volume is heated from radiation heat through the vessel wall, detector support structure and PMT heat loads. Sub-cooling of the xenon returning to the skin will therefore need to account for the increased heat loads in the skin region.

The subcooler also plays an important role during cooldown of the detector. During cooldown operations, xenon gas will be circulated through the system and the subcooler thermosyphons and their copper fins will gradually cool the circulating gas. Once the detector has reached base temperature, the subcooler thermosyphons liquefy xenon gas to fill the detector.

6.4.3 LXe transfer lines

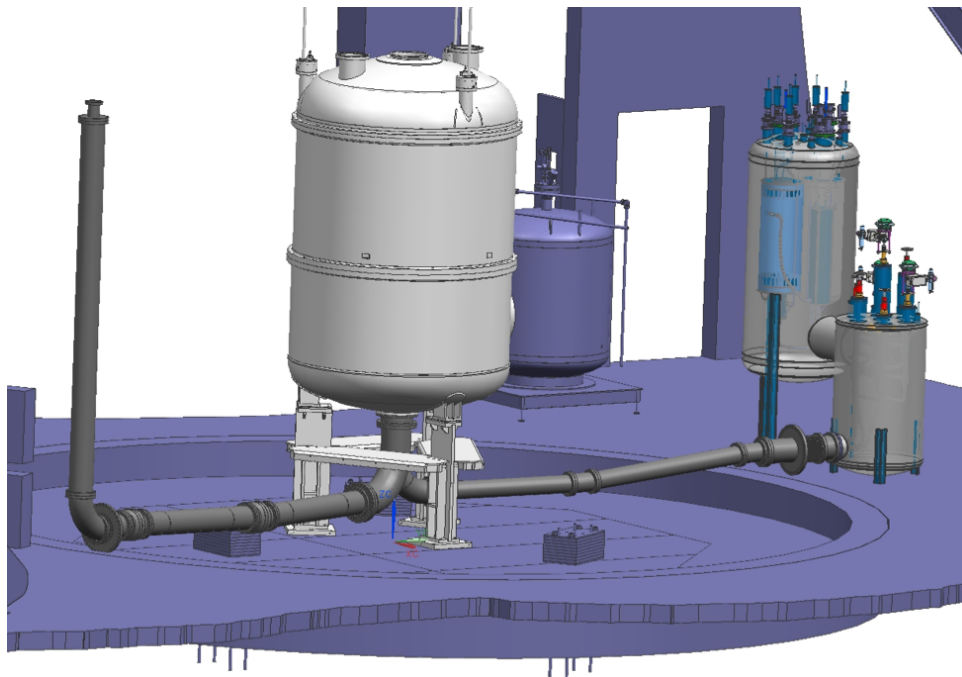


Figure 6.4.7: The TPC cryostat (center), the PMT cable standpipe (left), the LXe Tower (right), and the two vacuum insulation assemblies that house the LXe transfer lines.

As shown in Figure 6.4.7, two vacuum insulated assemblies host cryogenic lines that service liquid xenon to and from the cryostat at its lower flange. These two assemblies meet at a center Tee directly underneath the cryostat. Both are composed of sections of 8 inch tube and are assembled inside the water tank and sealed to its wall with flanged connections on opposite sides of the tank.

One of these assemblies, on the right side of Figure 6.4.7, houses the LXe supply and return for the primary circulation path of the online purification system. This assembly hosts two lines that route purified LXe from the subcooler to the skin and TPC active region, and a third line that connects the weir drain lines to the weir reservoir. These three lines are individually insulated with multilayer insulation because they can be at different temperatures. Connections will need to be made in these lines during assembly. While it would be ideal to make welded connections with an orbital welder, there may need to be VCR fittings to allow these connections to be made due to space constraints. A vacuum break is planned just after the center Tee below the cryostat. This helps provide protection in case of a leak and would also allow softening the vacuum in the transfer line region to add heat during Xe recovery. The weir drain line will be actively cooled

by a conductive connection to a thermosyphon. This will sub-cool the returning liquid below saturation temperature to decrease the possibility of vapor lock.

The second assembly, seen on the left side of Figure 6.4.7, houses the PMT and sensor cables from the TPC bottom PMT array. These cables exit the bottom of the detector cryostat, and are housed in a 4 inch ID bellows reinforced with a braid. The flange at the bottom of the inner cryostat has a connection for both the bellows housing the cables and the LXe lines. The cables are pulled into the bellows in the reduced radon clean room of the surface assembly lab and the bellows is sealed for transport underground to keep the cable clean. During lowering of the inner cryostat into the outer cryostat the lower cable bellows is pulled through the tee in the center bottom of the water tank. The shape of the Tee is designed to help guide the cable bellows. The multilayer insulation for this line is wrapped around segments of 180 mm OD polyethylene tube that is supported from the inside of the 8 inch SS tube with plastic thermal standoffs.

The final section of the cable path is the vertical PMT standpipe that is located outside the water tank and connects to the bottom of the breakout box. The standpipe is shown on the left side of Figure 6.4.7. The liquid level in the PMT stand pipe is about the same as the liquid level in the detector. The liquid is cooled with evaporation by pumping xenon out of the gas space above the liquid surface. The xenon gas between the liquid and the bottom of the breakout box has a temperature transition to room temperature.

As noted in Section 6.4.5, the upper and lower PMT conduits and the high voltage conduit will extract a total of 2.0 slpm of xenon gas through the PMT cable breakout boxes. This ensures that flow with the higher level of contamination from the plastic is always out of the detector where it is cleaned in a radon trap before it is returned to compressor suction. Both the liquid and vapor PMT cable runs will have a flow restrictor as close as possible to the outer flange of the cryostat. The restrictor is designed such that the Peclet Number (advection/diffusion) $\gg 1$. For the liquid line this means a collar around the cables for several inches reducing the size of the big gaps.

6.4.4 SLAC System Test prototype of the circulation architecture

Previous experience with the LUX cryogenics and its xenon handling system is only partially applicable to LZ due to the increased complexity of the LZ design. To exercise the new architecture, a large System Test platform containing over 100 kg of LXe has been developed at SLAC, including an extensive xenon handling capacity to purify LXe to realistic levels. As shown in Figure 6.4.8, the platform emulates most of the critical design features of the LZ architecture. It implements a separated LXe tower, containing a weir reservoir, a subcooler, and two-phase and single-phase heat exchangers, and it is connected to the TPC by vacuum insulated LXe transfer lines. These elements perform the same functions that their counterparts will in LZ, although their designs are not identical. Purified liquid is delivered to the bottom of the TPC and is recovered from the top via a weir spillover. That liquid is routed to the LXe tower by draining into a vertical pipe that penetrates the inner cryostat and descends to the bottom of the TPC vessel in the insulating vacuum space.

Several test runs of the circulation system have been carried out, and after some exploration of the thermodynamic parameter space and some hardware fixes, uniform flow at a rate of up to 75 slpm has been achieved for more than 80 consecutive hours. This provides a proof of principle that the LZ circulation architecture is viable. Under the conditions of uniform flow, the liquid level in the TPC is set by the weir spillover as desired, and the reservoir and sub-coolers are filled with a constant (but flowing) volume of buffer liquid. Data from these circulation tests provide a benchmark for engineering models of the two-phase heat exchangers in both the System Test and LZ.

The System Test has also highlighted some challenges presented by the LZ design, particularly the vacuum insulated weir drain line. We have found that, under some conditions, the flow of the saturated LXe in this line can be interrupted. Both the geometry of the line and the heat leak into it may be responsible for this

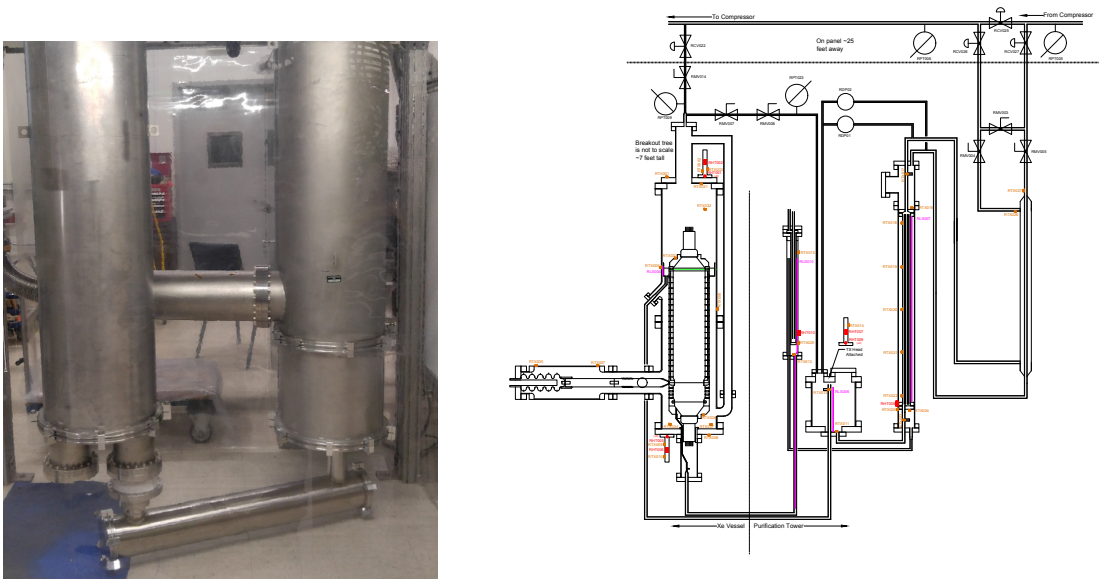


Figure 6.4.8: Left: System Test LXe tower vessel (left vertical vessel) and TPC cryostat (right vertical vessel), connected by vacuum insulated LXe transfer lines housed inside the lower horizontal vessel. Right: Schematic diagram of the internal elements. At left is the TPC, serviced by a large horizontal HV feedthru, and instrumented with one PMT on top and on bottom. The small vessel in the lower middle is the weir reservoir. It is surrounded by the sub-cooler and the two-phase and single-phase heat exchangers. The vacuum insulated transfer lines are below.

behavior. We are exploring the addition of active cooling to the line to counter this effect, so that uniform circulation can be stably achieved under a variety of pressure and temperature conditions.

6.4.5 Radon removal

Material screening is the primary route to control the ER and NR backgrounds resulting from radioactivity in the experiment. Recent estimates of radon emanation from PMT HV cables, cable feedthroughs and cable conduits, shown in Table 6.4.1, however, suggest that ^{222}Rn backgrounds may be up to 37 mBq, which is substantially above required levels. It is therefore required to mitigate radon with a combination of cable cladding and radon removal for the xenon gas circulation system. Neither action alone is sufficient. Adding 150 μm FEP cladding to the braided PMT HV cables will greatly reduce the risk of dust or other surface contamination in the steel braiding of the cables and essentially eliminate emanation from the cables in LXe, but will have no effect on PMT feedthroughs. Adding a radon trap with a volumetric gas flow of $\phi=2$ slpm in the (warm) gas circulation system will eliminate 90 % of radon from cables and feedthrough, but will have no effect on the PMT HV cables immersed in LXe.

Removal of radon from xenon is challenging due to the similar atomic diameters of these two species (120 pm vs. 108 pm, respectively [9]). However a pioneering demonstration of such removal at $\phi=1$ slpm has been performed by the XMASS collaboration using a cooled column of activated charcoal [10]. This result has been reproduced in Ref. [11] at $\phi=0.25$ slpm.

To determine feasibility of radon removal in xenon gas for LZ, a series of elution curve measurements were performed to determine the breakthrough time, τ , (i.e. adsorption coefficient) of radon in xenon carrier gas at various temperatures with a 30 g activated charcoal trap, since studies [12] of ^{222}Rn adsorption in gases

Table 6.4.1: Radon emanation estimates for PMT HV cables, cable conduits and cable feedthroughs. Also shown are estimates for including only cladding or a charcoal trap, as well as combining both mitigating methods. With only initial measurements of PMT feedthroughs available at this point, estimates for the other components are based on similar items of materials from other experiments. All estimates are in mBq.

Item	Component	Radon Emanation			
		estimated	w/ cladding only	w/ trap only	w/ cladding & trap combined
PMT HV Cables	warm insulation	0.27	0.41	0.027	0.04
	warm braiding	1.88	0.47	0.19	0.05
	warm dust	13	0	1.30	0
	cold insulation	2.7×10^{-4}	4.1×10^{-4}	2.7×10^{-4}	4.1×10^{-4}
	cold braiding	1.88	0	1.88	0
	cold dust	13	0	13	0
PMT HV Cables	Subtotal	30.0	0.88	16.4	0.09
Cabling Conduits	warm & cold	0.1	0.1	0.055	0.055
PMT Feedthroughs	warm	7.3	7.3	0.73	0.73
	Total	37.4	8.3	17.2	0.87

(other than air [13]) are scarce. Breakthrough time is given by $\tau = \frac{m \cdot k_a}{\phi}$, where k_a is the dynamic adsorption coefficient, m the mass of charcoal, and ϕ the volumetric gas flow.

Figure 6.4.9 (left panel) shows breakthrough time versus inverse temperature of radon in xenon carrier gas with a 30 g activated charcoal trap. Although a linear relationship is expected over the entire temperature range in the semi-logarithmic representation shown in Figure 6.4.9, the deviation from linearity may reflect Xe saturation on the charcoal surface.

Based on the elution curve measurements, a 90 %-efficient radon removal element for the xenon gas circulation system was designed as shown in Figure 6.4.10. The size of the charcoal trap was determined to be 8.6 kg (i.e. 19 liters) by scaling up the elution curve measurements with the small trap ($m=30$ g, $\tau=156$ min, $\phi=0.5$ slpm at -68 °C) to $\tau=12.7$ days (i.e. 3.3 half-lives), $\phi=2$ slpm and -85 °C. This can be accomplished with two 1 m-long columns of 3 inch diameter connected in series.

Gaseous xenon from the purge-gas line conduits will be introduced into the radon removal system through a SAES high temperature getter before it passes through the charcoal trap. The charcoal trap will be immersed in a cryostat vessel that is filled with HFE-7100 coolant and kept at a temperature of -85 °C using a EK-90 refrigerator or a thermosyphon. The system will allow transmission of xenon gas with flow rates ranging from 0 slpm to 2 slpm using a diaphragm circulation pump.

To measure the amount of radon in the carrier gases, a Si PIN photodiode (ORTEC) made from low radioactivity components will be used. The electronics readout will consist of a 142AH ORTEC preamplifier with low noise and fast timing characteristics as well as little temperature dependence, and a shaping preamplifier. A multichannel analyzer (ORTEC MCA-2K) will process the signals from the preamplifier. The radon system will be fully automated using high pressure pneumatic valves, and pressure and temperature sensors that are integrated into the LZ slow control system.

To validate the design and perform studies with different trap geometries using various adsorbents at various flow rates, a separate full-scale prototype system has been designed and built at the University of Michigan that makes use of the final cryogenics system. Initial measurements with the prototype system

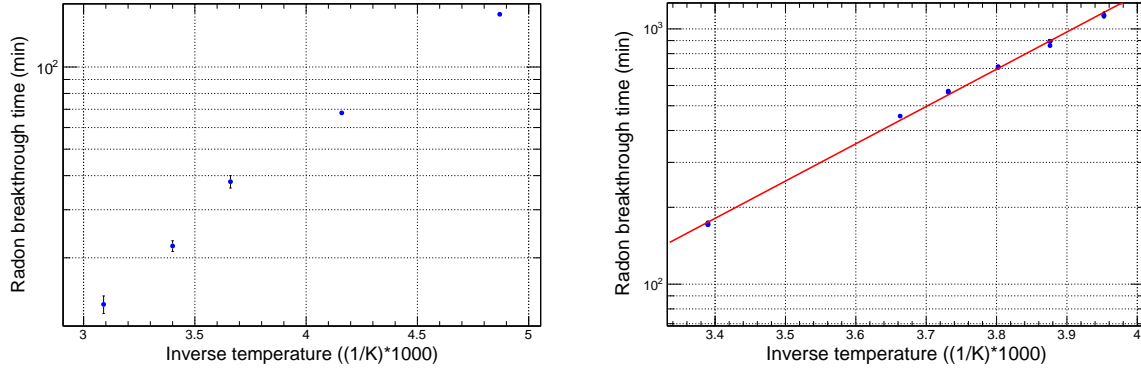


Figure 6.4.9: Radon breakthrough time versus inverse temperature for two different configurations. Left panel: Breakthrough time in a 30 g charcoal trap with a Xe carrier gas at a flow rate of 0.5 slpm. Right panel: Breakthrough time in a 50 g charcoal trap with nitrogen carrier gas at a flow rate of 2.0 slpm. The red line is a fit of the data to the Arrhenius equation $r = A \exp\left(\frac{E_a}{RT}\right)$, with r the inverse breakthrough time, A the collision frequency factor, T the temperature, E_a the activation energy, and R the universal gas constant. The fit values are $A = 0.00187 \pm 0.00044 \text{ min}^{-1}$ and $E_a/R = 3375 \pm 65 \text{ (K)}$. Note that the temperatures in the traps are known to about $\pm 1 \text{ K}$.

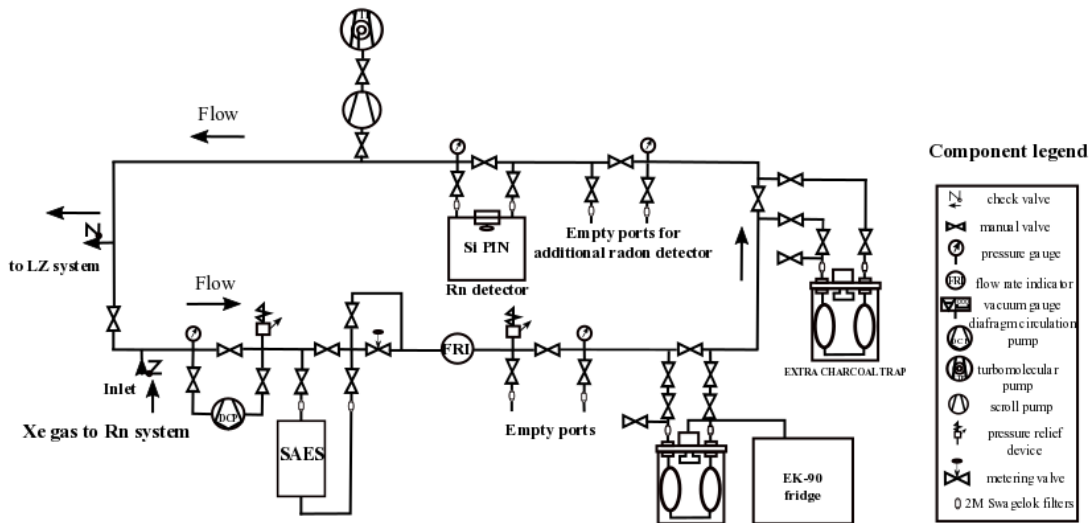


Figure 6.4.10: Schematic diagram of the radon removal system for LZ.

are underway. The right panel of Figure 6.4.9 shows the breakthrough time of radon in nitrogen carrier gas versus inverse temperature in a 50 g charcoal trap. The system will soon be operated with argon or helium gas before expensive xenon gas is used as carrier gas. It contains a radon calibration source to study the adsorption efficiency of the traps with different adsorbents besides natural carbon and different amounts of the adsorption materials. The test system can be used to study the adsorption efficiency of radon traps in a broad range of temperatures and trap geometries. The traps can be swapped and regenerated by baking and pumping at high temperatures.

6.4.6 Slow controls

A set of industrial Programmable Logic Controllers (PLCs) will handle instrument read-out and control for the xenon purification and recovery systems, as well as the cryogenic and systems and TPC high voltages (excluding PMTs). The PLC logic will include interlocks protecting the integrity of the xenon system, control loops and automated procedures for the various subsystems, and automated emergency response. All PLC programming will follow IEC 61131-3 standards.

The overall PLC system architecture includes one top-level PLC plus smaller dedicated PLC's for large equipment items, namely the cryogenerator system and four xenon compressors (2x recovery and 2x circulation), see Figure 6.4.11. The top-level controller is a Siemens S7-410-H Redundant Hot Backup PLC, which includes redundant processors with independent links to I/O modules. The redundant processors guarantee bumpless switchover in the case of processor failure, and also allow for zero-downtime when updating PLC logic and I/O mapping. The Siemens S7 PLC system will have a dedicated internally redundant APC Symmetra UPS as well as parallel DC power units for the S7 cpu's and I/O power, ensuring uninterrupted control when switching to generator power.

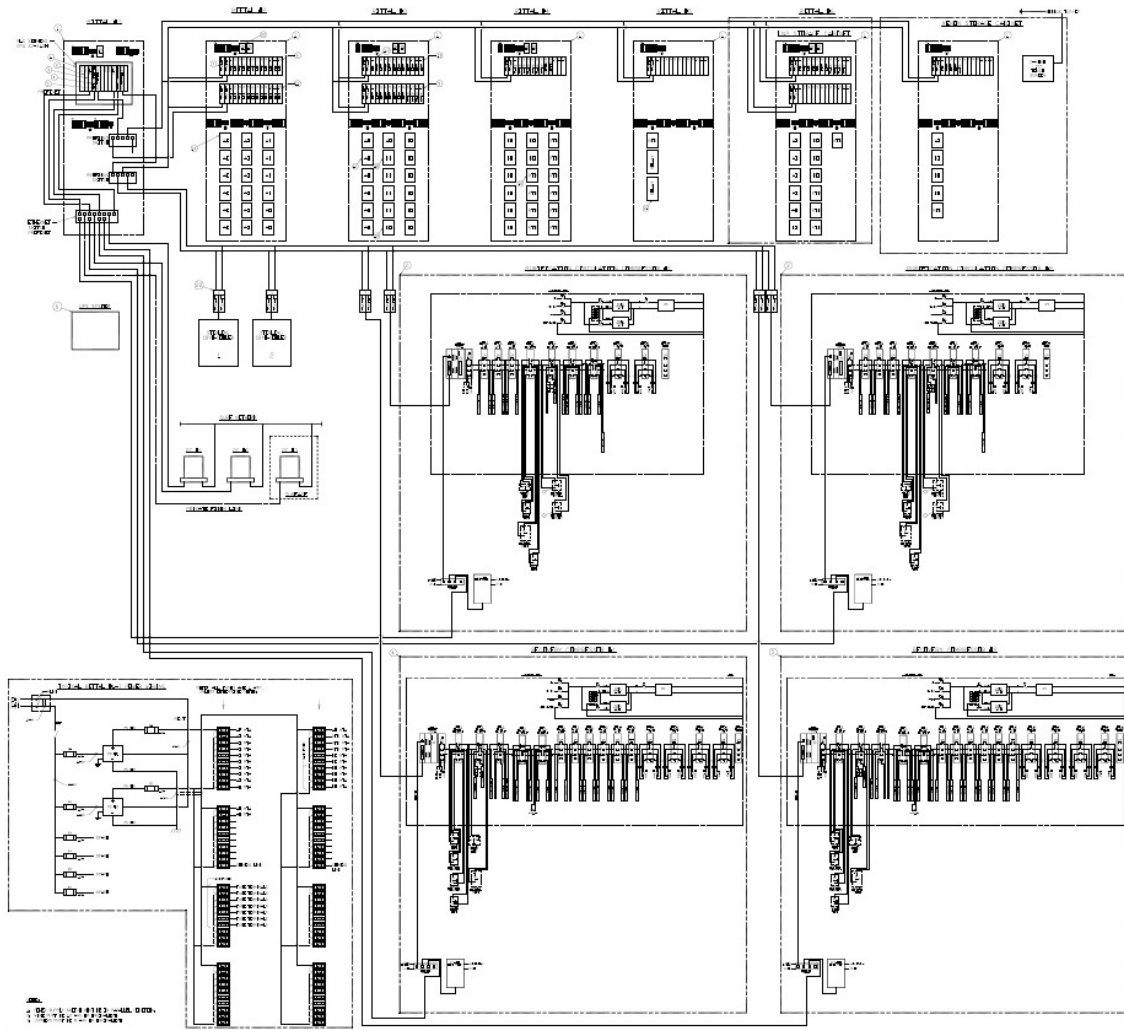


Figure 6.4.11: Block diagram for the PLC System.

All instruments not directly related to compressor or cryogenerator control will be read-out/controlled by the S7 PLC. This amounts to an estimated 832 channels of I/O, including 144 thermometers, 192 other Analog Inputs, 80 Analog Outputs, 80 Discrete Inputs, and 336 Discrete Outputs. The S7 logic will handle all interlocks and control loops relating to these instruments, in addition to top-level decision making for the compressor and cryogenerator systems. The S7 PLC will also be responsible for accomplishing xenon recovery in the event of a prolonged power outage (see Section 6.5). The S7 PLC will connect to the LZ Slow Control system via an Ignition Server on the PLC private network (see Section 8.8). The PLC network will receive power from the PLC UPS system and will have a direct, redundant fiber link to a backup server in the surface facility, ensuring monitoring and control capability in the event of power and network failures (see Section 8.12).

Each compressor skid will have a dedicated Beckhoff CX8031 PLC that will handle interlocks protecting that compressor, automation of compressor start-up and shut-down, and control loops to regulate flow rate and pressure at the compressor inlet. The Beckhoff PLCs on the recovery compressors will have the additional ability to independently initiate emergency xenon recovery if the TPC pressure exceeds a set threshold (See 6.5). All variables in the Beckhoff PLC logic will be exposed to the Siemens S7 via Profibus, and in normal operations the Beckhoff PLCs will receive high-level commands (start/load/unload/stop) from the S7 over the Profibus connection. In this way the S7 also serves as the gateway between the compressor PLCs and the LZ Slow Control system. A touch-screen human-machine-interface (HMI) on each skid will allow each compressor to be operated as an independent unit when disconnected Siemens S7.

The liquid nitrogen generation system will have a vendor-supplied Siemens S7-300 Series PLC with local HMI to control the Stirling cryogenerators. As with the compressor PLC's, all variables in the PLC logic will be exposed to the main Siemens PLC via Profibus, providing the same monitoring and controls as are available through the vendor-supplied HMI.

6.5 Xenon Recovery

The Xe recovery system removes the Xe from the detector and returns it to the storage cylinder packs. There is also a regulator-based Xe delivery function in the opposing direction to support detector cooldown and condensing.

The xenon recovery system must support three functions: 1) Normal recovery, such as a planned full recovery at the end of the experiment or for small operational adjustments of xenon quantity in the system, 2) Emergency recovery, where the xenon is automatically removed from the system and safely stored during an unexpected sustained pressure rise or extended power failure, and 3) Venting xenon as a last resort to provide detector MAWP⁷ pressure protection. With the exception of function 3, in all scenarios the xenon asset must be retained and its purity kept intact. The system also offers online cryopumping and cryogenic buffer volume that can absorb small pressure spikes, xenon feed and bleed to various points throughout the system, and redistribution of trace xenon.

At the heart of the recovery system is a pair of recovery compressor skids. The skids are redundant replicates, each one containing all the hardware necessary for autonomous recovery, including valves, sensors and interlocks, Beckhoff PLC controller, and the compressor itself. Both compressors are commanded to run when activated in an emergency. Compressor suction is connected directly to the detector ullage, isolated by a pneumatic shutoff valve to allow for independent compressor startup routines. A discharge-to-suction proportional bypass valve provides variable flow, using compressor suction pressure as feedback. Once operating, the compressor is controlled to maintain constant suction pressure - this way the compressors only transfer the xenon being fed to them. The compressors themselves are all-metal triple-diaphragm two-stage

⁷Max Allowable Working pressure

LZ Xenon Recovery System High-Level Schematic

20161020 TLB

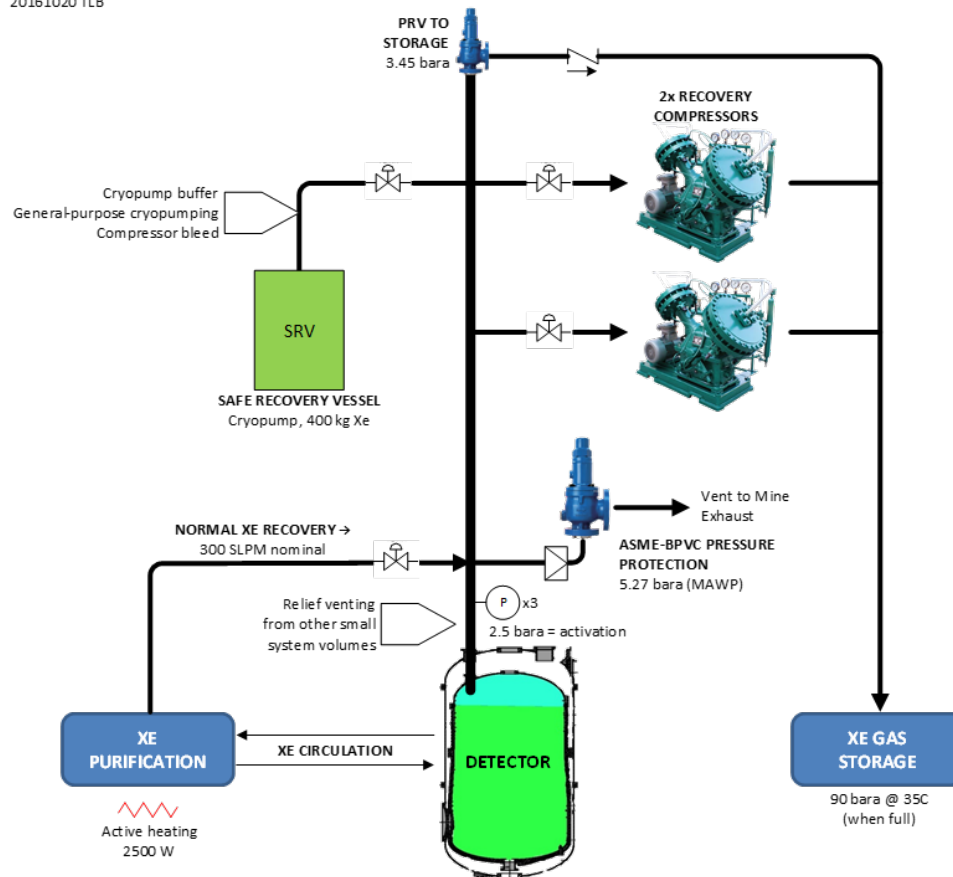


Figure 6.5.1: Simplified flow schematic of LZ Xe Recovery system.

compressors, each rated for 350 slpm at 2.5 bara suction pressure (automatic recovery activation pressure), and 100 bara discharge. A simplified flow diagram of the recovery system is shown in Figure 6.5.1.

All pressure relief mechanisms throughout the xenon handling system are vented into the detector ullage, which acts as a gaseous buffer. Here the vented gas either condenses in the detector or can be stored/removed by the recovery system. A set of cryo vessels tap off the main delivery and recovery gas trunks. The larger vessel is the SRV (Safe Recovery Vessel) repurposed from LUX, and has a xenon capacity of 400 kg and maximum pressure rating of 83 bara (1190 psig). This vessel is nominally maintained cold at xenon ice vapor pressure, 1.0×10^{-3} mbar, allowing it to act as an online cryopump buffer to absorb small pressure spikes within the detector and also bleeding of xenon from various points throughout the xenon handling system. A smaller cryopump consists of two 4 L research bottles with a combined xenon capacity of 15 kg, and can be used in conjunction with the SRV to redistribute trace xenon by way of volume sharing.

Automatic emergency xenon recovery is a layered approach and illustrated in Figure 6.5.2. The automatic recovery trigger is keyed to the detector ullage pressure, which is monitored by three pressure transducers. All three communicate to the main Siemens PLC, two of them via the dedicated compressor skid Beckhoff PLCs. Detector operating range is 1.6 to 2.2 bara. A set of alerts are issued from the control system once detector pressure reaches 2.2 bara. At 2.5 bara, and a 2/3 vote between the three pressure transducers, automatic recovery is activated. If the pressure continues to rise to 2.8 bara, each Beckhoff controller assumes the

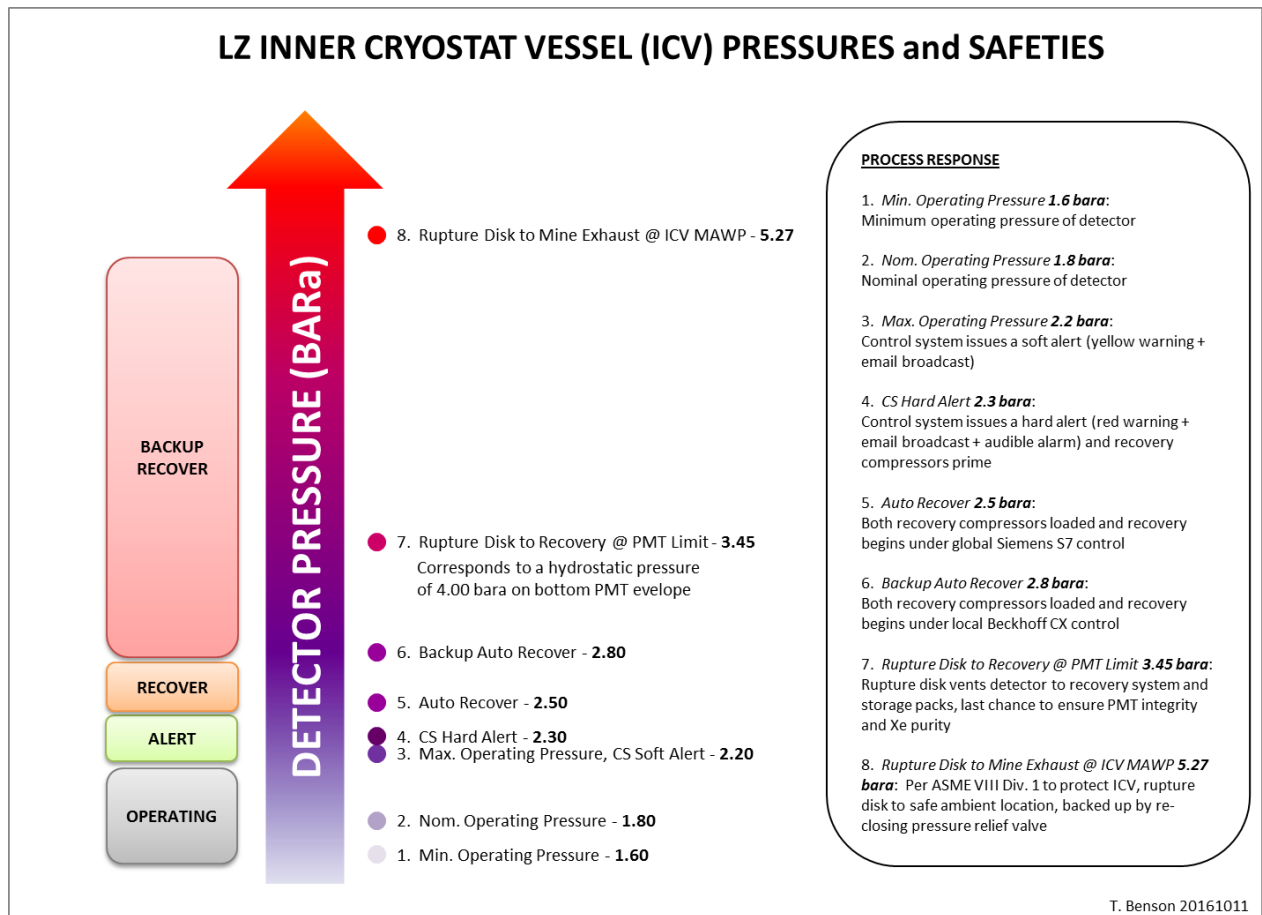


Figure 6.5.2: Xe system pressure threshold plot.

main PLC has failed to initiate recovery and commands its own skid to begin recovering autonomously. At 3.45 bara the bottom PMTs are at risk of failure from hydrostatic pressure. At this point it is assumed the compressors are not functioning, or not functioning fast enough, and a pressure relief valve vents the detector to the evacuated storage cylinders in hopes that this is a transient spike and not a continuous rise in pressure. Finally, as a last resort to protect the cryostat against rupture, a rupture disk vents xenon to mine exhaust at 5.27 bara (detector MAWP). This burst disk is backed up by a re-closing pressure relief valve so all remaining xenon can be retained after the pressure event is resolved. In this case some xenon is lost, the system purity is compromised, and some PMTs have possibly mechanically failed.

See Figure 6.5.3 for P&ID details of how the recovery system elements and detector tie together. The full P&ID for the core system is shown in Figure 6.5.4.

An analysis of various failure scenarios drives the recovery system design and sizes the compressors. Specifically, our worst case scenarios would be an air or water breach of the vacuum jacket insulating the detector and LXe transfer lines, an air-breach being the more probable of the two. We first address these failures by specifying a layer of foam insulation to be applied to the outside of the inner cryostat vessel wall and bottom head (all vessel surfaces wetted by liquid xenon on the other side). The insulation is specified to have a maximum heat transfer coefficient (k/t) of 3 W/m² and 1.5 W/m² for the wall and bottom, respectively. Second, we include vacuum breaks on the lower transfer lines to isolate such a failure and minimize the effected heat transfer surface area.

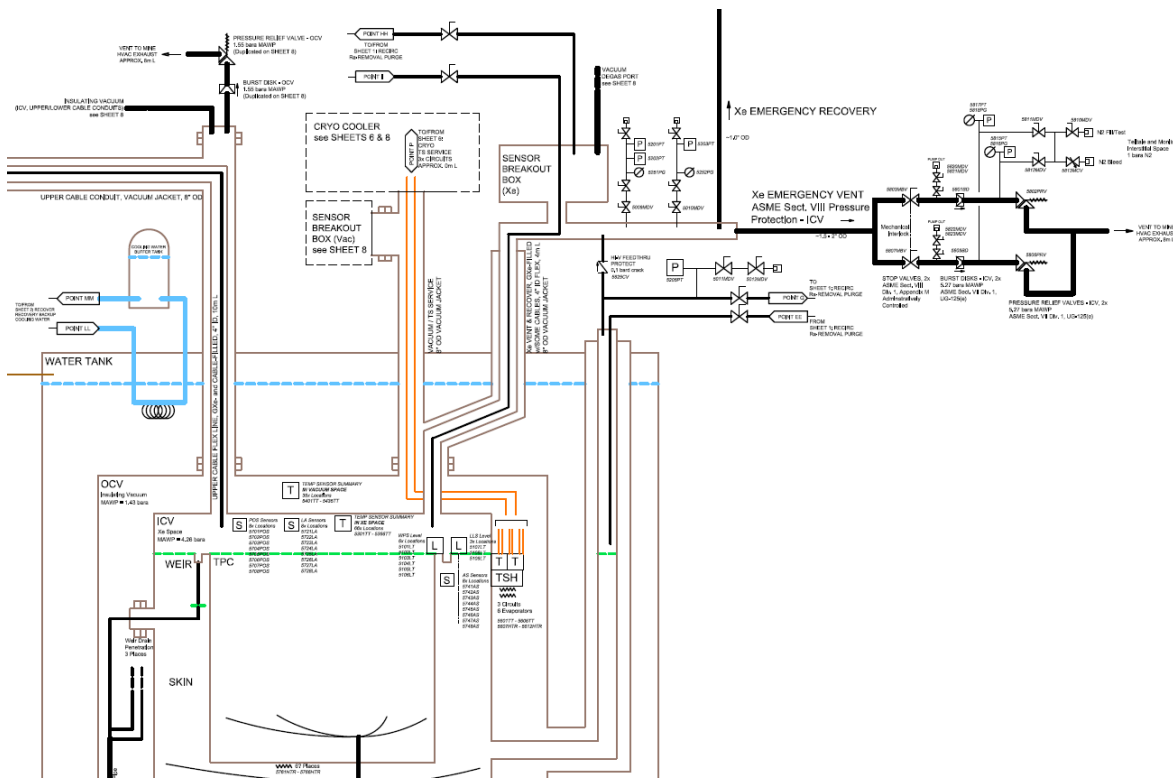


Figure 6.5.3: P&ID detail of how the recovery system ties into the detector. The main recovery path out of the detector is via a 4 inch ID bellows containing a small bundle of sensor cables. This path is instrumented with redundant pressure transducers, and both the main recovery line and the ASME ICV pressure protection tap into this line.

With the above design provisions in place, a conservative dynamic model was developed to estimate heat loads for the air and water breach cases. From these, initial boiloff rates are in the range of 400 slpm and 2,500 slpm for the air and water cases, respectively. Boiloff tapers as the LXe level in the detector drops, and significantly tapers in the water case as a layer of ice forms and grows. Then, by looking at the detector pressure response versus time for various sizes of compressors, and making sure it always stays below safe limits, we are able to choose an optimal compressor size. Note that compressor throughput is a strong function of suction pressure, so at higher suction pressure the compressors will move more gas, and vice versa. On a first-order this means the compressors self-regulate to match boiloff, and detector pressure is a function of how much xenon is being removed, or in other words what size the compressors are. Physical size is also a factor since underground space is extremely limited. From this analysis, one 350 slpm compressor (at 2.5 bara suction pressure) can handle the more probable air-breach case, and two of these same compressors running in parallel can handle the water-breach case. Since the analysis is conservative, these compressors will be slightly over-sized for the application, which makes it important to have variable flow capability by way of the proportional bypass valves on the compressor skids.

Normal recovery is driven by electric heaters that actively heat and boil the xenon in a controlled manner. These heaters are located in the bottom of the LXe Tower on the LXe supply lines leading to the detector (Figure 6.4.6), and are sized to deliver a combined 2,500 W to boil off xenon at a rate of 300 slpm. Once normal recovery is initiated, main circulation stops and the recovery heaters begin boiling off xenon at the bottom of the LXe Tower. Flow through the supply lines is reversed from normal operations: LXe is draining out of the detector and flowing towards the heaters while xenon boiloff travels up through the subcooler and

out a gas extraction line. This extraction line plugs into the input of the gas recirculation loop. From there, the xenon can be routed directly to the recovery compressor inputs, or can first be pushed through the getter one last time before storage (this requires the circulation compressors to be operating to overcome the getter's impedance). Again, the recovery compressors operate on constant suction pressure control, and as more gas is liberated into the gas plumbing the recovery compressors transfer it out. Assuming a constant 300 slpm removal rate, full recovery would take approximately 4.2 days.

There are also design provisions for a more passive recovery strategy. Here, a low-elevation cold-to-warm liquid tap at the bottom of the LXe Tower is normally blocked off by redundant shutoff valves. Upstream of the valves (but at lower elevation) there is a room temperature heat exchanger. With this approach, LXe drains out of the detector and into the heat exchanger where it is boiled off. The boiloff gas is routed back into the detector ullage, where it both recondenses onto the liquid surface and helps raise the bulk xenon temperature over time, and raises detector pressure as gas builds up. The pressure buildup will eventually trigger the emergency recovery routine. This backup approach may be helpful to supplement and/or kick-start a full xenon recovery if there is a need to recover faster.

Two underground generators provide backup emergency power to the experiment: 1) A SURF 300 kW generator, and 2) An LZ 40 kW generator. Within one minute of a power outage, the large generator automatically starts and sustains ventilation and critical experimental operations in the Davis Campus. At this time, non-critical LZ loads are systematically shed while critical loads are maintained, including backup cryogenic cooling and any functions relating to xenon recovery. The large generator is coupled with a 1,000 gallon fuel tank and is able to sustain ventilation and critical experiment loads for approximately 3 days. During this time, a high-level decision can be made whether to initiate a full xenon recovery or wait. If a decision is not made, or if outside communications have been severed, the recovery system will automatically initiate a full recovery after a predetermined amount of time after the power loss. This is to ensure the xenon is safely stored before there is no fuel left to do so. When a low fuel condition is detected on the large generator, and power has still not been restored, the smaller LZ generator (coupled with a 270 gallon fuel tank) begins warming up. The large generator then runs out of fuel, and within 10-20 ms an automatic transfer switch transfers the load to the LZ generator. The recovery system plans ahead for the switchover by briefly shutting down the compressors and then restarting after the switch is complete. On the other hand, the control system is carried through all switchovers by their UPS units. Assuming all recovery loads are active while the LZ generator is running, and that it started with a full 270 gallons of fuel, it will continue running for approximately 4 days. The combined run time of both generators is 7 days, and it takes 4 days for a normal full recovery.

6.6 Long-term xenon storage and transportation

The LZ Xe will be sourced from multiple gas suppliers (Section 6.9), shipped to SLAC for krypton removal (Section 6.3), shipped to SURF to be moved underground, and finally liquefied into the LZ detector. Vendor-grade Xe arrives at SLAC in vendor-supplied gas cylinders. Once krypton has been removed, the Xe is stored and transported in special high-integrity gas cylinder packs specifically engineered for LZ. The Xe storage, transport, and transfer must be done without any loss of the high-asset xenon, and must also meet or exceed the overall storage inbound leak rate requirement of 1.15×10^{-6} mbar l/s (helium) as specified in Section 6.2.1.

The LZ cylinder packs conform to DOT 49 CFR Part 178, Subpart C, Specification for Cylinders. Base packs will be purchased as turnkey items from Praxair, with modification and final integration and testing occurring at the University of Wisconsin's Physical Sciences Laboratory (UW-PSL). There will be 12 gas cylinder packs available to contain the full 10 tonnes of Xe for LZ (see Figure 6.6.1 for some features of the LZ cylinder pack design). Each pack contains 12 DOT-3AA-2400 49.1 liter cylinders, each having a working pressure of 166 bara (2,400 psig). The full quantity of Xe can be stored in all 144 cylinders in a

LZ XENON STORAGE PACK

TLB 20161024

DOT 49 CFR Part 178, Subpart C, Specification for Cylinders

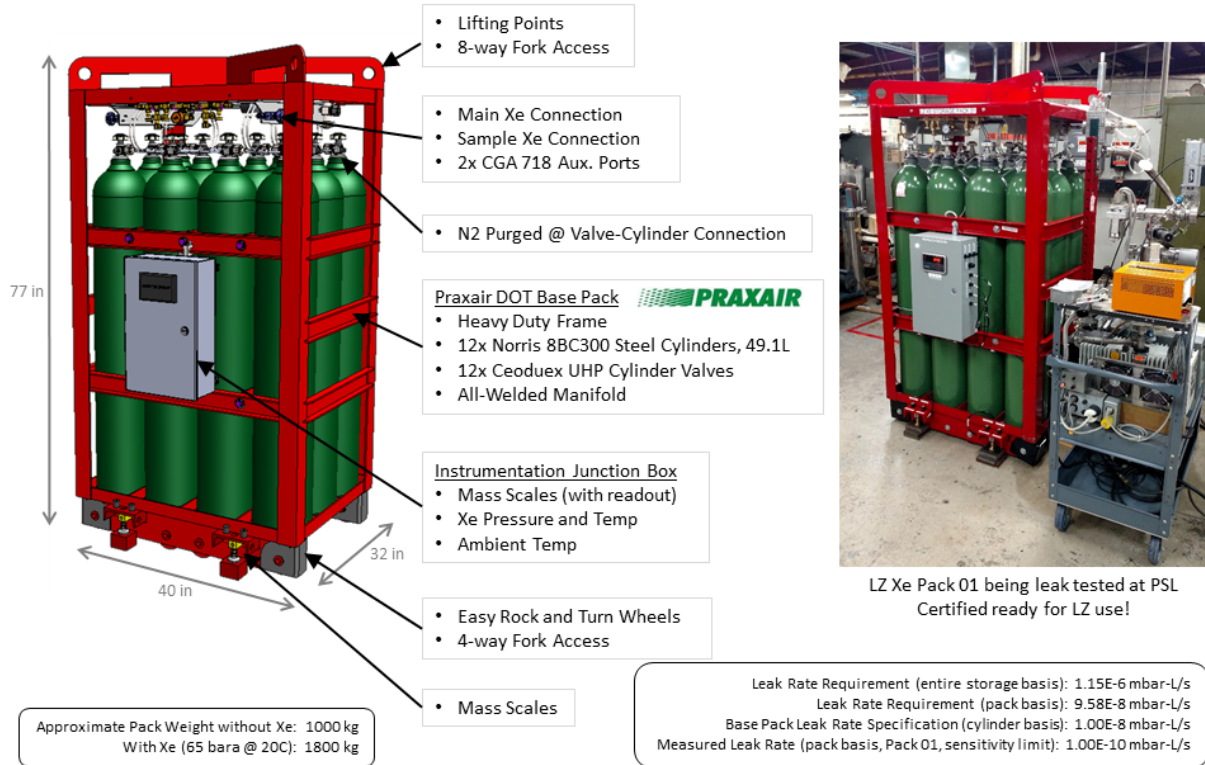


Figure 6.6.1: Overview of LZ cylinder gas pack.

supercritical state at a pressure of 65 bara (928 psig) at 20 °C. Each cylinder then contains approximately 69 kg (12,700 standard liters) of Xe and each full pack weighs a total of 1,800 kg. The maximum allowable Xe charge into these cylinders for transport per DOT regulations (pressure must be below 5/4 working pressure at 55 °C) is 91 kg (this would require at minimum 110 cylinders). The 65 bara target storage pressure offers a favorable packing density on the Xe density curve near its critical point (16.6 °C, 58 bara) without placing excessive output pressure requirements on the compressors needed to fill the packs.

The cylinder valves are equipped with a pressure burst disk rated at 277 bara (4,000 psig) per DOT specification. In the event of a fire, with 69 kg of Xe charge, this pressure would be reached at a temperature of 136 °C. If the burst disk failed to vent, the cylinder burst pressure of 398 bara (5,760 psig) would be reached at a temperature of 202 °C.

Particular attention is given to the seal between the valve and the cylinder. Economics drives us to use a standard NGT (National Gas Taper) thread that is readily available from DOT cylinder manufacturers. This seal can represent the weakest link in the system from a leak-tightness perspective. The requirement that the total leak rate be no more than 1.15×10^{-6} mbar l/s implies that the average inbound leak should be less than 9.6×10^{-8} mbar l/s into each of the 12 packs, and less than 8.0×10^{-9} mbar l/s into each of the 144 cylinders. To achieve this we set a target inbound helium leak rate of 1×10^{-8} mbar l/s for each of the cylinders, while we further reduce Kr ingress by flushing the volume immediately surrounding the NGT seals with boil-off nitrogen from the cryogenic system. We believe the flushing can reduce the Kr ingress rate of Kr by a factor of 10 over ambient air. During storage we also benefit from a favorable high pressure gradient between the

stored Xe and outside ambient conditions, however this effect is not present during operations when the packs are empty. After integrating the base pack into the final LZ design at UW-PSL, a leak check is performed on the entire pack, including the manifold, to certify it ready for LZ use. For these tests, the leak checking system is first calibrated with a calibrated helium leak.

Considerable R&D has been carried out in collaboration with Praxair's R&D Division on achieving our target specification. Initially we tested two valve/cylinder pairs, and have since received and tested the first complete LZ storage pack. Initial factory leak rates range from $9.0\text{e-}8$ to $4.1\text{e-}9$ mbar-L/s, but then after pumping down for a few days to reduce helium background in the cylinders, measured leak rates drop dramatically. In particular, for the first LZ pack, Storage Pack 01, the helium leak rate was measured to be less than $1.0\text{e-}10$ mbar-L/s, the sensitivity limit of the leak test equipment. Two valve thread preparation techniques were compared: 1) standard practice of PTFE tape with Krytox applied above the 5th thread, and 2) thin layer of indium plating, 0.002 inch and 0.004 inch thicknesses were both trialed. A metal-metal seal must be achieved with the NGT thread in order to meet LZ's allowable leak rate requirement, and the purpose of the valve thread preparation is to allow full engagement and deformation of the NGT threads without onset of galling. The indium seemingly has the advantage of flowing to fill any gaps with metal, however results of all 14 cylinders (2 R&D cylinders + 12 cylinders in first pack) suggest both techniques work, and in fact the PTFE results were slightly better. The most important factors for achieving a good seal is careful thread inspection and gauging prior to installation, and that installation be performed by an experienced technician. All valves for the LZ storage packs will be installed by experts at Praxair, and the remaining valves will be prepared using the standard PTFE tape technique per Praxair's procedures.

We have selected Ceodux D304 UHP tied diaphragm valves with CGA 718 (DISS) output connection type. The cylinders in a pack are manifolded together with an all-welded stainless steel manifold with VCR xenon connection taps and instrumentation ports for a pressure gauge and transducer. Xe gas line temperature is monitored and also ambient temperature within each pack. The packs are supported by scales that monitor xenon mass to an accuracy of ± 0.23 kg. Xe temperature and pressure, ambient temperature, and weight of each pack is read out to the PLC system. The pack frame is a rugged steel frame equipped with fork-access both on bottom and top, rigging pick points on top, and retractable wheels.

Transport of the Xe packs will be divided into approximately 3 to 4 separate shipments, both to match the Kr-removal production schedule and to reduce risk of total xenon loss in the event of a serious road accident. The shipments will be insured, and will travel in secured air-ride trucks.

Once at SURF, the packs will be moved underground as soon as possible to limit cosmogenic activation of ^{127}Xe . The packs will be loaded on a small rail car in the Yates headhouse, loaded into the cage, lowered to the Davis Campus level, and rolled into the Davis Campus on a rail car. Part of the Davis Campus infrastructure work is to prepare a Xe Storage Room for the Xe using an existing excavation in the LN storage room access drift, as shown in Figure 6.6.2. In order to maintain clearance beneath the HVAC and sprinkler utilities in the access drift, the cylinder packs may need to travel horizontally. In this case, a specially-designed pack rigging fixture will assist in the rotation and handling of each pack from the Yates headhouse to the underground Xe Storage Room. We are investigating an alternative and preferred option to instead modify the utility services so that the packs may travel in their upright configuration. The Xe Storage Room will be sealed from the access drift with a block wall and secured double doorway.

The Xe Storage Room will have a boil-off nitrogen supply to purge the valve seal volumes, a sprinkler system to control temperature during a fire (activates at 68°C), and an emergency ventilation and oxygen monitoring system in case of an accident. Supply and return plumbing from the Xe storage area will connect the packs to the LZ detector plumbing via a gas panel equipped with a sampling/pump-out bus and local cryopump (15 kg Xe capacity) for consolidating xenon locally. Xe Storage Room controls are supported by a local PLC control rack on UPS and backup power. Portable provisions for clean sampling of various

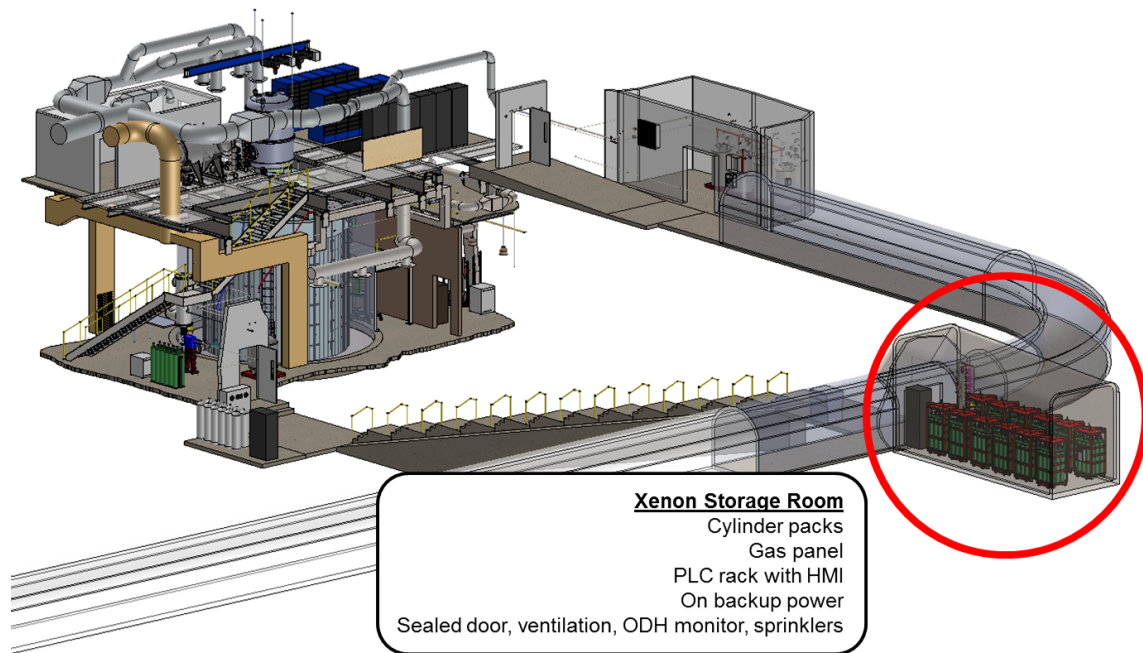


Figure 6.6.2: Location of the Xe Storage Room in the Davis campus, along the access drift to the LN2 Storage Room.

locations within the Storage Room will also be provided. A complete P&ID of the integrated Xe storage plumbing is provided in Figure 6.6.3.

Once the Xe has been fully transferred into the LZ detector and Xe handling system, any xenon remaining will be consolidated to a single pack and the remaining packs will be maintained under vacuum and ready to accept incoming Xe from any recovery action.

6.7 Xenon Sampling and Assay

Sensitive Xe purity monitoring is integrated into the Xe handling plan. The basic monitoring methodology that we employ is the coldtrap/mass-spectrometry method developed for LUX and EXO-200 [6, 14]. The LUX experience is reviewed in Ref. [15]. In this section we describe the LZ implementation.

The method works as follows. A gaseous Xe sample flows through a precision vacuum leak valve or MFC to an RGA, where the partial pressures of the various species are measured. Once a uniform flow is established, these partial pressures are proportional both to the abundances in the sample and to the gas flow rate, and inversely proportional to the volumetric pumping speed of the vacuum system at the RGA. The partial pressures can be interpreted as absolute concentrations by calibrating the measurement under specified flow and pumping conditions with Xe gas samples prepared with known impurity content.

Good sensitivity may be achieved by maximizing the gas flow rate and minimizing the pumping speed, however the total pressure cannot exceed about 10^{-5} torr if the RGA and its electron multiplier are to function well. Without additional measures the Xe partial pressure would severely limit the flow rate, so the Xe is selectively removed by passing the gas sample through an LN coldtrap where it forms Xe ice. Under these conditions the Xe partial pressure at the coldtrap outlet is held at 1.8×10^{-3} torr, the vapor pressure of Xe ice at 77 K. This is still too high by a factor of 180, however the Xe pressure may be further reduced at the

RGA by inserting an appropriate impedance into the plumbing. In the presence of the coldtrap the Xe partial pressure at the RGA does not depend on the gas flow rate into the trap.

Some impurity species (such as water) are removed from the gas stream by the coldtrap and are thus unobservable at the RGA. However, many species of interest pass through the trap with good efficiency, including O_2 , N_2 , CH_4 , Ar, He, and, most importantly, Kr. Studies have shown that the partial pressures of these species continue to be a good measure of their concentrations as long as an appropriate calibration is done at a similar flow rate and vacuum pumping speed.

In contrast to Xe, the partial pressure of Kr at the RGA is found to be much less sensitive to the vacuum impedance between the coldtrap outlet and the RGA. It decreases only moderately as the impedance increases, allowing Xe to be selectively suppressed relative to Kr. The origin of this unusual behavior is that the Xe signal is a pressure source created by the Xe ice in the coldtrap, while the Kr signal is a current source created by the gas flow into the coldtrap.

This distinction in the nature of the Xe and Kr signals is advantageous because Xe dominates the total pressure and thereby limits how low the pumping speed may be set without exceeding the RGA's pressure limit. After Xe suppression, however, the pumping speed may be further reduced, increasing the partial pressures of all species, including Kr and Xe, until Xe once again reaches the RGA's practical limit of 10^{-5} torr. In practice, vacuum parameters such as the impedance and pumping speed are not modified during a run but are instead chosen for optimal sensitivity in prior test runs. The resulting system configuration may be calibrated as usual with specially prepared Xe gas samples with known krypton content.

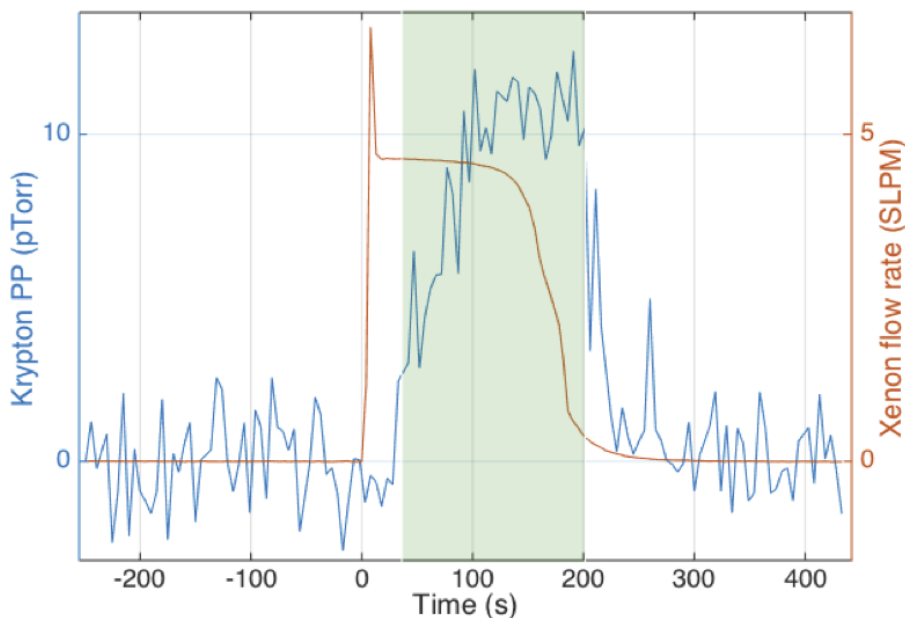


Figure 6.7.1: Blue: Kr partial pressure trace at a concentration of 0.34 ppt (Kr/Xe) (g/g) (left vertical axis). Orange: Flow rate into the cold trap in (slpm, right vertical axis). The green shaded region is the signal integration window.

Empirical studies have shown that the efficiency to pass Kr through the coldtrap depends upon its tubing diameter, with smaller diameter tubing generally performing better. Another important factor is the total amount of Xe ice that can be collected before the flow path becomes blocked. Larger ice capacity implies

that a larger flow rate may be sustained for the same time period, further enhancing the Kr signal. For LZ we have adopted a 0.5 inch OD tube as a baseline compromise between these competing needs.

To improve the Kr sensitivity of the method beyond the 0.2 ppt achieved for the LUX Kr removal campaign, we have increased the mass flow rate by a factor of four from ~ 1.5 slpm to 6.5 slpm and decreased the pumping speed by a factor of five from ~ 5 to 1 liters/sec. We've also implemented an MFC for better programmable flow control. Results are presented in Figure 6.7.1, where a prominent Kr partial pressure signal is shown for a Kr concentration of 0.34 ppt (Kr/Xe) (g/g). Studies of the sensitivity of the method, performed with Kr-free xenon gas samples, have found that the limit of detection is 0.007 ppt (g/g) (Kr/Xe) at 90%C.L.

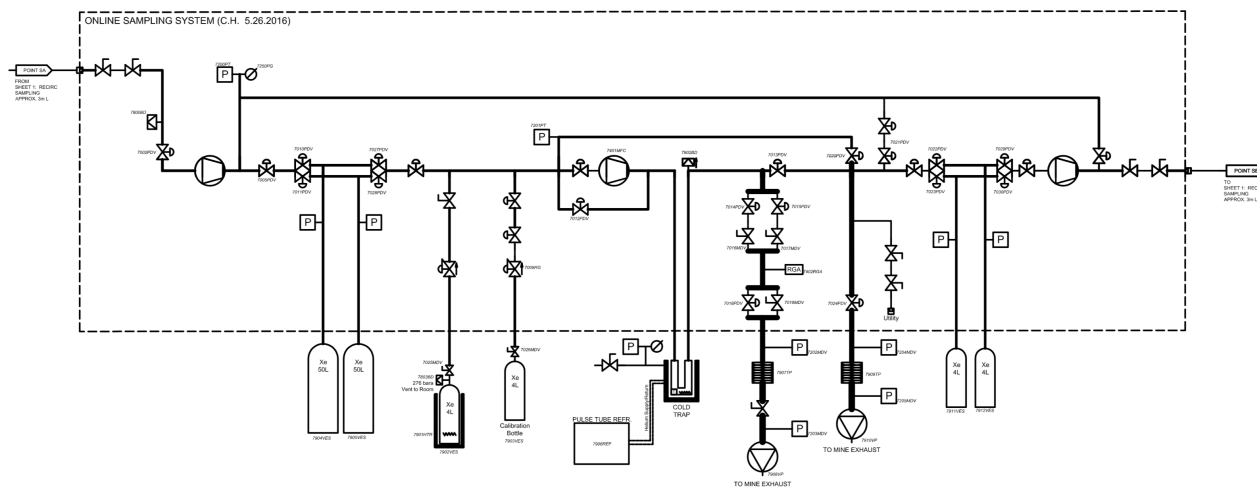


Figure 6.7.2: P&ID of the LZ online Xe sampling system.

An analytical system incorporating these design features has been constructed at SLAC to aid the Kr removal campaign described in Section 6.3, and to perform quality assurance on the vendor-supplied xenon as it is acquired. The SLAC system is currently integrated into the R&D chromatography system, and will be re-purposed for use in the production system in 2018.

At the conclusion of krypton removal operations, the SLAC sampling system will be shipped to SURF and be permanently integrated into the LZ xenon circulation system at the Davis campus. A P&ID of this system is shown in Figure 6.7.2. To simplify continuous operations at SURF, the coldtrap will be cooled by a pulse-tube refrigerator as shown in Figure 6.7.3, and accumulation bottles on the input and output will allow xenon gas to flow continuously through the system. The LUX sampling system will also be re-built and re-purposed at SURF as a mobile utility sampling system for use during detector commissioning and operations.

6.8 Cryogenics, vacuum services, and breakout boxes

This section describes the design of the liquid nitrogen cryogenic systems. We also describe here the vacuum pumping systems and the breakout-box feedthroughs for the internal PMT and instrumentation cables.

Cooling power to maintain Xe in the liquid phase is provided by a cryogenic system that distributes nitrogen in gas and liquid phases. By utilizing the approximate 100 K temperature difference between the nitrogen and Xe evaporation temperatures, sufficient gradient exists to provide for thermal control and temperature

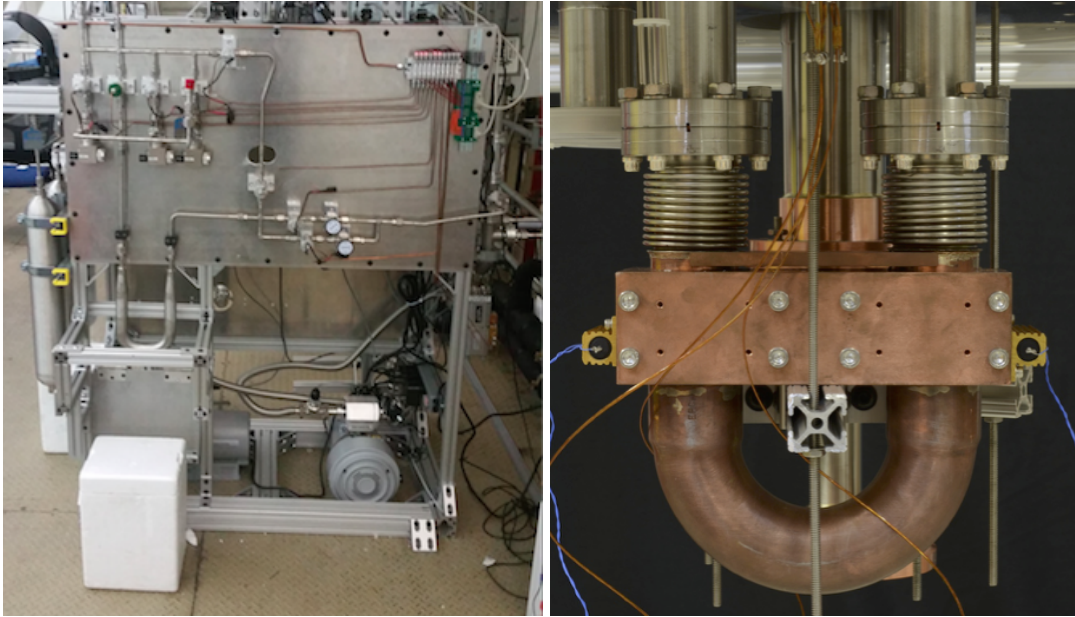


Figure 6.7.3: Left: Xe sampling system constructed at SLAC in 2015 for monitoring Kr removal activities and screening the commercially procured Xe stockpile. Right: Prototype copper coldtrap with temperature control provided by a pulse tube refrigerator coldhead.

modulation. Existing infrastructure from LUX, including 450-liter LN storage tanks; vacuum-jacketed (VJ) pipe; and miscellaneous valves, sensors, and fittings are modified and re-utilized to provide a front end to the primary cooling equipment for the experiment while providing supplemental LN storage. During operations, distribution of LN is from a VJ central 750-liter distribution tank that is co-located with a Stirling cycle cryocooler. The cryocooler liquefies cold evaporated nitrogen gas in a closed-loop cycle operating at near atmospheric pressure. Multiple thermosyphon heat pipes, cooled by the LN in the storage tank, are used as heat sinks to provide for heat removal from the Xenon system. Primary heat removal locations are the detector, high-voltage feedthrough, and the LXe tower. The underground installation is shown in Figure 6.8.1

Exterior to the Davis Cavern is an LN storage room that contains four 450-liter LN storage tanks installed on mass scales that monitor LN consumption. A commercially purchased vacuum-jacketed (VJ) piping system that has a complete implementation of control valves, relief valves, and pressure-monitoring equipment connects the tanks to equipment in the Davis Cavern. Separate small-diameter tubing connected to the storage tanks distributes boil-off nitrogen purge gas for the freeboard of the water tank, the water-purification system vacuum pump, the scintillator reservoir, radioactive source deployment systems, and Xe equipment protected from radon leakage. The four storage tanks are required to provide an initial liquid volume for startup of the cryocooler, meet high load transient conditions, and provide backup to the cryocooler until a second cryocooler procured at a future date. Alterations to the VJ piping system are required to allow for rerouting of LN to new destinations in the Cavern that will differ from the LUX LN use locations. The rail-mounted 1,100-liter LN storage tank utilized by LUX will provide for the resupply of LN from the surface during brief cryocooler operation interruptions and periodic replenishment of consumed purge gas.

A cryocooler based on the Stirling thermal cycle is selected for cooling of LZ. It is depicted schematically in Figure 6.8.2. Included in the cryocooler design is a cryogenerator, a work platform sized for two cryogenerators, a 750-liter LN storage tank to provide a distribution reservoir, and a complete monitoring and control system. The design of the cryocooler is closed cycle. Nitrogen inside the storage tank is re-liquefied rather than being vented to the cavern as was done during LUX operations. The cryocooler is capable of 1,000 W

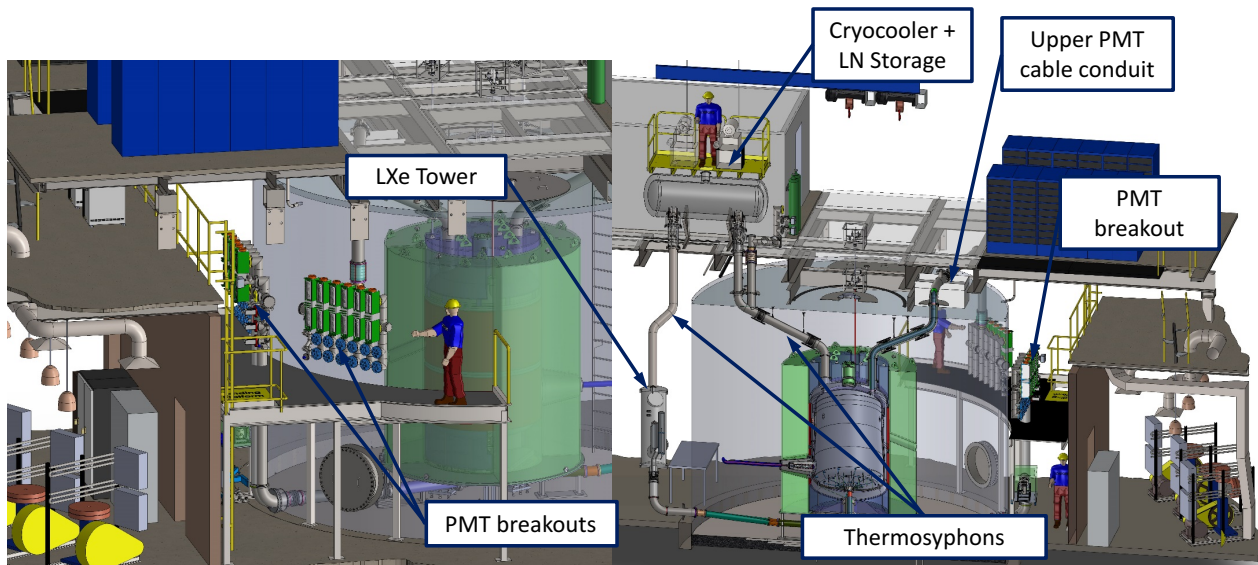


Figure 6.8.1: Cryogenics installation in the Davis Cavern.

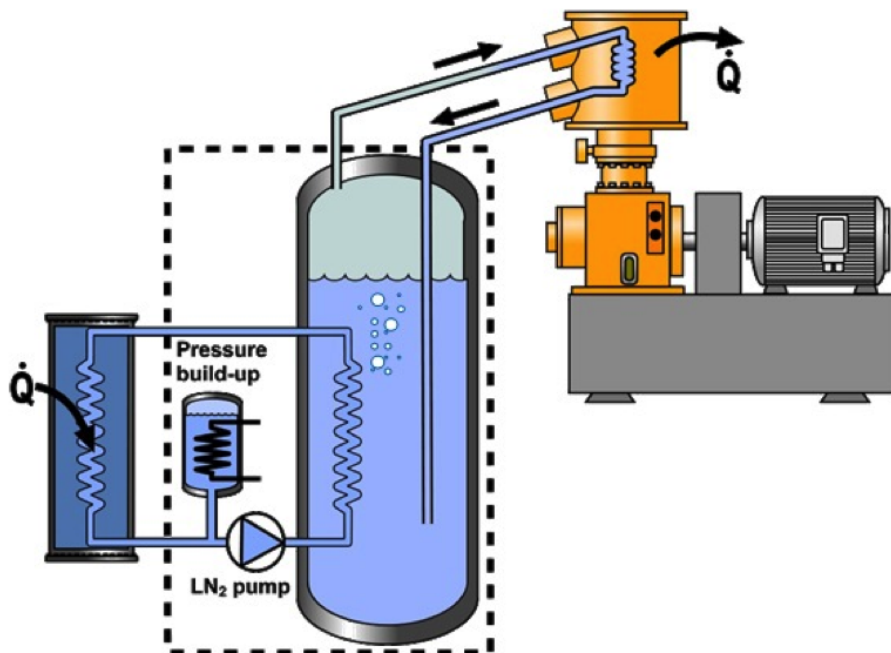


Figure 6.8.2: Cryocooler schematic. A cryogenerator removes heat, Q , from a closed liquid nitrogen storage reservoir. Other devices requiring heat removal are thermally connected to that reservoir. All of the systems are closed-loop.

of cooling power at the 77 K boiling temperature of LN at atmospheric pressure. Preliminary estimate of total heat load on the cryogenic system is 838 W including 20 % contingency. The heat load rollup is shown in Table 6.8.1. The 1,000 W configuration provides a margin against unanticipated heat load.

Table 6.8.1: Heat load rollup.

System/Component	Heat (W)	Notes
LZ cryostat	115	Assumes 10 liters of MLI; value confirmed by independent analysis in U.K.
PMT Conduit	34	
HV Conduit	1	
Cryocooler Storage Tank	28	Calculated for 1000-liter tank; value diminishes for smaller Dewars.
Heat Exchanger	349	Assumed at 94% efficient (LUX experience) @ 500 slpm Xe flow.
Xenon Purge	56	Estimate for 5 slpm flow rate.
Thermosyphons	116	Dominated by heaters; could go up for higher thermosyphon count.
Contingency @ 20%	140	
Total	838	

Cryocoolers based on the Stirling cycle have the additional advantages: quick startup, low energy consumption (each unit draws 11 kW of electricity), and variable drive motors that allow adjustable cooling levels below 1,000 W. These units have been deployed at many institutions worldwide, including installations at SNOLAB, Gran Sasso (Icarus), and multiple university laboratories in the United States, Russia, and Asia. Maintenance of the cryocooler is required after 6,000 hours of continuous use, so the system is designed for the future addition of a second cryocooler (likely purchased as a component of operations). Transport of LN from the surface to the Davis Campus can sustain operations during short-term maintenance that is expected to have a duration not exceeding 8-hours.

LUX has received deliveries of LN two to three times per week. Even though LZ is better insulated, scaling indicates that LZ requires one LN delivery every 24 to 36 hours to sustain operation. For long-term operations, that would increase the inherent transport risk and manpower requirements related to LN transfer. Therefore, the addition of a second cryogenerator at some point would significantly reduce the risk to long-term operations.

Distribution of cooling power from the cryocooler to the Xe-containing experimental systems is accomplished by use of thermosyphons. A thermosyphon is a type of heat pipe. Thermosyphon technology was successfully applied to LUX following development at Case Western Reserve University (now SLAC). Thermosyphons comprise condenser and evaporator heads connected by small-diameter tubing wrapped with multilayer insulation (MLI) and charged with nitrogen gas at modest pressure. In this application, the condenser is immersed in an LN bath, causing the nitrogen gas in the thermosyphon to liquefy. The liquid flows in the small-diameter tubing by gravity to the evaporator that is physically attached to the device that requires cooling. Heat from the evaporator causes the LN pooled in the evaporator to change phase, removing heat via the nitrogen latent heat of vaporization. The warmed nitrogen gas then returns to the condenser by buoyancy effect.

Cooling of the Xe relies upon the temperature difference between the LN and Xe vaporization temperatures as well as the adjustable cooling power of the thermosyphon. Changing the mass of circulating nitrogen can modulate the thermosyphon cooling power. As the mass is increased, pressure in the condenser rises, effectively increasing the boiling temperature in the thermosyphon and inducing an increased heat flux to the LN bath that remains at atmospheric pressure and 77 K.

Thermosyphon cooling is completely passive, with a fixed amount of nitrogen in the secondary cooling loop. Therefore no pumps are required and there is no direct path for large quantities of LN (typically stored in Dewars) to get into the Xe via a leak. As the thermosyphon transport tubing may be 9.5 mm or 12.7 mm OD, a minimal amount of nitrogen can be placed into the tubes, on the order of 15 g to reach 10 bara. This mass gradually increases as the nitrogen condenses but the mass remains modest. Over-pressure protection is by relief valves and burst disks. The thermosyphons are charged with nitrogen via high-pressure cylinders. Control of the gas mass (and cooling power) is accomplished with control valves, mass flow controllers, sensors, and processing devices connected to slow control via Ethernet. Thermosyphons deployed in LUX were easily capable of delivering more than 200 W cooling for each deployed evaporator head. The single largest device needing cooling is the LXe tower, in which two-phase, sub-cooler, and gas-gas heat exchangers are anticipated to require 349 W of cooling to recondense Xe returning to the detector. Three thermosyphon evaporators are able to provide that energy removal.

Vacuum-pumping systems take advantage of tubing in place to route thermosyphons, Xe transfer lines, and PMT cables. Packages of combined scroll pumps and turbo-molecular pumps are deployed on the decking of upper Davis Cavern and near the Xe heat exchanger tower in lower Davis Cavern. These pump combinations evacuate: the annulus between the inner and outer vessels, detector internals, Xe heat-exchanger tower, and the entire Xe gas system. Two vacuum leak check carts are provided so that there is a minimum of one cart available at any time in the Surface Assembly Laboratory and the underground Davis Campus. A variety of gauges are deployed, including manual gauges (that can show vacuum in power outage), thermocouple gauges, and ion gauges.

A critical element of vacuum pumping is removal of residual gases from detector internals that are either attached to metal surfaces or dissolved into plastic volumes. Empirical data developed at U. Maryland for gas solubility and diffusion in plastics is used along PTFE volume / thickness measurements from Solid-Works CAD models to predict the required vacuum pumping to achieve acceptable levels of Kr, N₂, and O₂. Predicted steps for vacuum pumping are as follows:

1. Pump detector to 1×10^{-4} torr and hold for one day;
2. Backfill with 10 torr Xe gas;
3. Circulate Xe gas that is heated to 40 °C for 45 days;
4. Pump out Xe gas and achieve 1×10^{-6} torr predicted to take 65 days;
5. Maintain that pressure at room temperature for one additional week.

By that time residual Kr in the detector is predicted to be less than 0.03 ppt with a pumping duration of 3.3 months.

PMT, sensor, and grid power supply cables from both the inner and outer cryostats must be routed to locations where they can transition from either a pure Xe or high-vacuum environment to atmospheric conditions in the Davis Cavern. These cables are routed through VJ conduits. Two conduits exit the cryostat from the top and one from the bottom. One upper and one lower conduit, primarily carrying PMT cables, are routed to a SURF-installed mezzanine level. Sensor and grid cables exiting the top of the detector are routed to the main Davis Cavern deck. The inner tube of the VJ is braided flexible conduit sized to allow pulling of all

cables during installation. The outer jacket has “tee” connections to the vacuum-pumping system. Stainless steel breakout boxes are installed on the conduits at the mezzanine and main Davis Cavern deck for installation of hermetic feedthroughs at the point where cables must be terminated in order to exit the Xe and vacuum spaces. Breakout boxes and inner conduits are compatible with the 3.4 bara maximum Xe pressure and meet Xe cleanliness requirements.

Control of temperature, pressure, and liquid levels within the cryogen system is needed both for the correct operation of detector systems and for safe operation. Control of these parameters is via connection to the slow control system described in Chapter 8. A detailed P&ID along with a related instrument list exists. Each thermosyphon utilizes multiple thermometers, pressure transducers, a vacuum gauge, a mass flow controller, and controller boxes to digitize signals and transmit via Ethernet. Similarly, the LN storage room, VJ distribution piping, cryocooler, and vacuum pumping system need active monitoring and control of temperature and pressure.

6.9 Xenon Procurement

Approximately 10 tonnes (1.8×10^6 gas liters) of Xe must be acquired for the LZ detector. The purity requirement is an industry standard of 99.999 % Xe. The Xe currently in the LUX detector and from small previous purchases will be reused (~90,000 liters). SDSTA initiated a bid and procure process for ~500,000 liters in the second half of 2015. Bids were requested and received from all major producers in the world and a few other sources with existing Xe stock. Delivery has started and will continue into 2017. A second bid cycle for up to about 1.2×10^6 liters was completed in February 2016 and deliveries have started. A fixed price and delivery schedule consistent with the LZ need to complete delivery by the end of 2018 was achieved. The University of Alabama has procured about 36,000 liters that have been delivered to SLAC. All Xe will be delivered to SLAC by the fall of 2018 for later removal of Kr. Approximately 20% of the LZ Xe has been received and assayed at SLAC, and all of it has met or exceeded purity specs.

6.10 Solubility and diffusion constants of common impurity gas species

To quantify the outgassing burden of the LZ TPC materials, the LZ R&D program produced a set of measurements of the diffusion and solubility constants of several common impurity species in various plastic and elastomer materials. Some result from that campaign were reported in Table 9.7.1 of Ref. [15], however, due to an editing error, portions of that table are incorrect. Table 6.10.1 presents the corrected values.

Table 6.10.1: Solubility (K) and diffusion constants (D) of common impurity species. K is defined as the ratio of impurity mass per unit volume inside and outside of the material sample. The PTFE sample is from the LUX TPC. PE1 is a polyethylene sample from LUX. The viton is an off-the-shelf sample from McMaster. PE2 is a polyethylene sample from a candidate cathode high voltage cable that was under consideration for LZ during its R&D phase. All measurements were performed at room temperature.

Solubility (K) (%)				
	PTFE	PE1	viton	PE2
N ₂	10.7 ± 0.7	2.1 ± 0.3	51 ± 10	
O ₂	22 ± 2	1.8 ± 0.6	22 ± 1	
Kr	58 ± 5	9.3 ± 1.1	23 ± 2	11 ± 2
Xe	89 ± 8	55 ± 6	15 ± 2	
Ar	8.8 ± 0.8	4.7 ± 1.5	8.3 ± 2.6	
He	3.3 ± 0.3	0.64 ± 0.07	9.3 ± 0.8	
CH ₄		16 ± 3		
Diffusion constant (D) (10 ⁻⁸ cm ² /s)				
	PTFE	PE1	viton	PE2
N ₂	15.1 ± 0.3	16 ± 1	2.2 ± 0.1	
O ₂	31.4 ± 0.6	39 ± 3	6.8 ± 0.1	
Kr	5.6 ± 0.1	6.4 ± 0.4	1.25 ± 0.02	11.2 ± 0.8
Xe	0.80 ± 0.02	2.0 ± 0.1	1.7 ± 0.1	
Ar	16.8 ± 0.3	20 ± 1	4.0 ± 0.1	
He	1270 ± 25	435 ± 30	436 ± 5	
CH ₄		6.6 ± 0.9		

6.11 Bibliography

- [1] H. H. Loosli, B. E. Lehmann, and W. M. Smethie Jr., in *Environmental Tracers in Subsurface Hydrology*, edited by P. G. Cook and A. L. Herczeg (Springer US, 2000) pp. 379–396, *Noble Gas Radioisotopes: ^{37}Ar , ^{85}Kr , ^{39}Ar , ^{81}Kr* , ISBN 978-1-4613-7057-4.
- [2] X. Du, R. Purtschert, K. Bailey, B. E. Lehmann, R. Lorenzo, Z.-T. Lu, P. Mueller, T. P. O’Connor, N. C. Sturchio, and L. Young, *Geophys. Res. Lett.* **30**, 2068 (2003).
- [3] R. A. Riedmann and R. Purtschert, *Environ. Sci. Technol.* **45**, 8656 (2011).
- [4] A. I. Bolozdynya, P. P. Brusov, T. Shutt, C. E. Dahl, and J. Kwong, in *Proceedings of the 11th Symposium on Radiation Measurements and Applications Ann Arbor, MI, USA 2326 May 2006*, Nucl. Instrum. Meth., Vol. **A579** (2007) pp. 50–53, *A chromatographic system for removal of radioactive ^{85}Kr from xenon*.
- [5] D. S. Akerib *et al.* (LUX), “Chromatographic separation of radioactive noble gases from xenon,” (2016), submitted to *Astropart. Phys.*, arXiv:1605.03844 [physics.ins-det].
- [6] A. Dobi, C. G. Davis, C. Hall, T. Langford, S. Slutsky, and Y.-R. Yen, *Nucl. Instrum. Meth.* **A665**, 1 (2011), arXiv:1103.2714 [astro-ph].
- [7] D. S. Akerib *et al.* (LUX), *Phys. Rev. Lett.* **112**, 091303 (2014), arXiv:1310.8214 [astro-ph].
- [8] A. Dobi, D. S. Leonard, C. Hall, L. Kaufman, T. Langford, S. Slutsky, and Y. R. Yen, *Nucl. Instrum. Meth.* **A620**, 594 (2010), arXiv:1002.2791 [physics.ins-det].
- [9] E. Clementi, D. L. Raimondi, and W. P. Reinhardt, *J. Chem. Phys.* **47**, 1300 (1967).
- [10] K. Abe *et al.* (XMASS), *Nucl. Instrum. Meth. A* **661**, 50 (2012).
- [11] S. Lindemann, *Intrinsic ^{85}Kr and ^{222}Rn Backgrounds in the XENON Dark Matter Search*, Ph.D. thesis, University of Heidelberg (2013).
- [12] K. Munakata, T. Fukumatsu, S. Yamatsuki, K. Tanaka, and M. Nishikawa, *J. Nucl. Sci. Technol. (Tokyo, Jpn.)* **36**, 818 (1999).
- [13] Y. Fukuda *et al.* (Super-Kamiokande), *Advanced computing and analysis techniques in physics research. Proceedings, 8th International Workshop, ACAT 2002, Moscow, Russia, June 24-28, 2002*, *Nucl. Instrum. Meth.* **A501**, 418 (2003).
- [14] D. S. Leonard, A. Dobi, C. Hall, L. Kaufman, T. Langford, S. Slutsky, and Y.-R. Yen, *Nucl. Instrum. Meth.* **A621**, 678 (2010), arXiv:1002.2742 [physics.ins-det].
- [15] D. S. Akerib *et al.* (LZ), (2015), Conceptual Design Report; LBNL-190005, FERMILAB-TM-2621-AE-E-PPD, arXiv:1509.02910 [physics.ins-det].